EVALUATION OF GRANULAR DISTRIBUTION AND PROPELLANT GRAIN LENGTH ON TRI-MODAL AMMONIUM PERCHLORATE SOLID ROCKET MOTORS

By

DANIEL VELASCO

Bachelors of Science in Mechanical and Aerospace Engineering

Oklahoma State University

Stillwater, Oklahoma

May 2020

Submitted to the Faculty of the
Graduate College of the
Oklahoma State University
in partial fulfillment of
the requirements for
the Degree of
MASTER OF SCIENCE
May, 2022

EVALUATION OF GRANULAR DISTRIBUTION AND PROPELLANT GRAIN LENGTH ON TRI-MODAL AMMONIUM PERCHLORATE SOLID ROCKET MOTORS

Thesis Approved:

Dr. Kurt Rouser

Thesis Adviser

Dr. Rick Gaeta

Dr. Khaled Sallam

Dr. Jamey Jacob

ACKNOWLEDGEMENTS

I would like to thank my committee members: Dr. Kurt Rouser, Dr. Rick Gaeta, Dr. Khaled Sallam, and Dr. Jamey Jacob for their valuable insight and advice throughout the course of this study. Additionally, I would like to thank the amazing graduate researchers and students of the Oklahoma State University Richmond Hill Research Laboratory, both past and present, especially Colton Swart, Garner Copher, Tanner Price, Trey Schinzler, and Chris Rathman for their willingness to provide assistance over the course of the Spring 2022 semester. Thank you to my parents, Hortencia and Jose Velasco, as they have helped guide me down a path towards success through their continued unwavering and unconditional love and support. I would also like to thank all of my brothers: Brian, Dennis, Sam, and Steve Velasco for always being there for me in any time of need. Lastly, thank you Emily Dougherty for all of the love and support over the course of my undergraduate and graduate studies as you have provided me with the confidence and stability I have needed in order to complete my studies here at Oklahoma State University.

Name: DANIEL VELASCO

Date of Degree: MAY, 2022

Title of Study: EVALUATION OF GRANULAR DISTRIBUTION AND PROPELLANT GRAIN LENGTH ON TRI-MODAL AMMONIUM PERCHLORATE SOLID ROCKET MOTORS

Major Field: MECHANICAL AND AEROSPACE ENGINEERING

Abstract: This paper presents an evaluation on the effects that variances in ammonium perchlorate particles size, total aluminum content ratio, and solid rocket motor geometry has on tri-modal ammonium perchlorate composite solid propellant (APCP) performance. The primary goal of this study is to observe variances in consistency of solid motor performance as a function of average ammonium perchlorate particle size, differing formulation ratios of fuel and oxidizer, and number of propellant grains present within the motor. Despite ammonium perchlorate's wide usage in civil and defense applications, its chemical thermal decomposition is largely not well understood. Additionally, once propellant grains have been cast, the only readily available and non-invasive way to quality check a motor is through comparison of theoretical and actual densities. Quality checks give an indication for the amount of imperfections that cause unpredictable variations in performance metrics related to thrust, burn time, and impulse. A stochastic study to characterize performance fluctuations related to the manufacturing of APCP was conducted. Performance variations were evaluated on a 54 mm diameter motor over three different combinations of 90 μm, 200 μm, and 400 μm ammonium perchlorate particle sizes with respect to 2 and 3 grain motor configurations. Variances in aluminum content were evaluated at an average ammonium perchlorate particle size of 261 μm in a 2 grain configuration. Small sample hypothesis variance testing of motor performance at a 90% confidence level suggests that 2 grain motor configurations and increased aluminum content significantly decreased variations in several motor performance parameters. Variations in ammonium perchlorate average particle sizes showed that fluctuations in performance parameters of peak thrust, average thrust, and burn time reduced at an average particle size of 230 μm. However, average particle sizes of 261 μm and 199 μm supported increased consistency with respect to total and specific impulse. Ensemble analysis supports the conclusions from hypothesis testing as thrust profiles at higher aluminum contents, 2 grain motor configurations, and 230 μm ammonium perchlorate average particle sizes exhibited less average deviations and increased thrust profile consistency.

TABLE OF CONTENTS

Chapter Page

Chapter Page

LIST OF TABLES

Table Page

Table Page

Table Page

LIST OF FIGURES

Figure Page

Figure Page

Figure Page

Figure Page

CHAPTER I.

INTRODUCTION

1.1 Introduction and Motivation

Solid rocket motors are commonly used within civil and defense applications such as in several types of military ballistic missiles, the booster stages in orbital launch vehicles, missions requiring rocket assisted takeoff (RATO), and within the sphere of amateur high powered rocketry. In order for these rockets to be effective, it is important that their motor performance be consistent for ease of predictability. Performance of rocket motors is very dependent on materials, procedures, and overall composition levels from which their propellant is made from. Propellant variations within the same type of formulation and motor geometry will affect motor performance. The reduction of these propellant variations typically coincides with the ability to minimize air-pockets formed during manufacturing. Thus, bringing true propellant density as close to theoretical is most desirable. Ammonium perchlorate (AP) is widely used as an oxidizer for many composite solid motors and is the typical oxidizer of choice for high powered rocketry applications here at Oklahoma State University. Figure 1 below severs as reference for size and scale of high powered rocketry testing conducted here at Oklahoma State University.

Figure 1:Oklahoma State University High Powered Rocket Testing

Solid rocket motors are typically used within the first stages of launch vehicles, in particular ammonium perchlorate composite propellant (APCP) type motors are the only form of solid propellant currently used in orbital rockets. The type of APCP used includes an ammonium perchlorate oxidizer along with an aluminum powder fuel that is then mixed and held together through a hydroxyl-terminated polybutadiene (HTPB) binder [1]. Combining this particular formulation's relevancy to industry with APCP no longer being heavily regulated under federal explosive laws, presents the opportunity for increased research to be had in the area of APCP performance reliability. This makes the focus of this study being to observe the effects of APCP performance consistency relative to varying propellant composition and motor configuration.

Ammonium perchlorate formulations that use a single granular size of ammonium perchlorate have proven to result in inconsistent motor performance attributed to propellant densities that are much lower than ideal. It has been well documented that introducing multiple particle sizes of ammonium perchlorate will improve propellant density, as visualized in Figure 2 below, but a parametrized study relating a formulation's granular size to performance repeatability needs to be had. Thus, a study of the effects that oxidizer particle size has on solid composite motor performance is critical to characterizing the potential improvement to be had on motor consistency for future predictability. Additionally, the applicability of this potential improvement in motor performance consistency needs to be observed when overall propellant composition and motor geometry is varied.

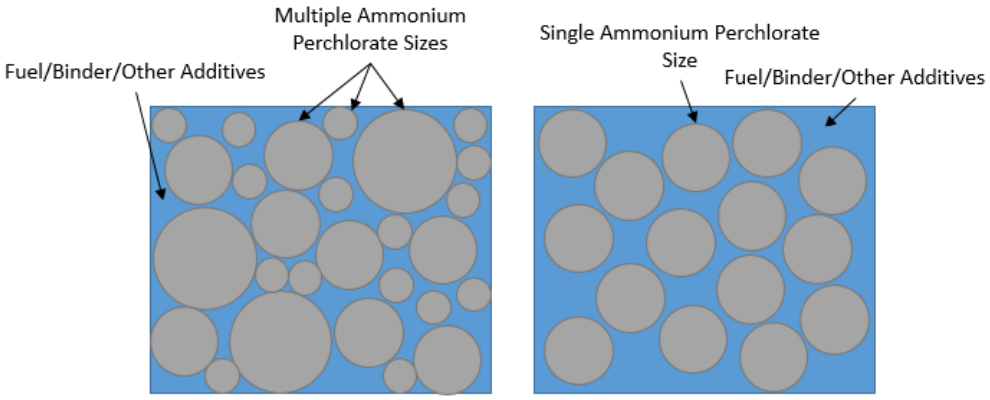

Figure 2:Multiple vs Single AP Size

Granular distribution within a propellant's composition may improve consistency of performance through the mitigation and prevention of air pockets, cracks, and other deformations that occur during solid propellant mixing and casting. An increase in these deformations brings an increase to the overall total burning surface area. A motor will perform significantly different due to the higher chamber pressures that are present with this unexpected and uncontrolled increase in burning surface area, making it difficult to predict performance characteristics like peak thrust, burn time, and specific impulse. Typical benchmarking for quality assessment of propellant density in order to get a sense for how many of these deformations could be present can be observed in Table 1 below [2].

Table 1: Density Ratio Quality Assessment Table [2]

Density Ratio	***Assessment***
1.00	Ideal only, not realizable in practice
0.95-0.99	Very good to excellent quality, essentially no voids or porosity
0.90-0.94	Fair to good quality, some porosity, voids, or other flaws
0.85-0.89	Low to marginal quality, significant porosity or flaws. If density ratio is low due to hidden flaws, grain should be discarded
<0.85	Serious flaws exist. Discard

1.2 Research Objectives

The Oklahoma State University high powered solid rocketry program has developed and progressed from relatively small 38 mm (1.50 in) diameter motors consisting of KNSB propellant, to an APCP formulation reaching motor dimeters of 76 mm (3.00 in). This large

increase in motor size has also translated towards observed peak thrust values ranging between 10 to 25 lbf with 38 mm motors, to upwards of 500 lbf and even instances where over 600 lbf thrust values have been recorded for 76 mm motors. Figure 3 below depicts the casings used for each motor size to serve as reference for this increase in scale.

Figure 3: 76mm (Left), 54mm (Middle) & 38mm (Right) Rocket Casings

All APCP related rocket motors manufactured and tested at Oklahoma State University have been mono-modal, consisting of only a singular size of ammonium perchlorate particles, and only through the use of a singular formulation. This particular formulation was chosen because it performs similarly to a composite propellant available preset within OpenMotor. This has allowed for convenient and rough modeling of expected performance metrics. This mono-modal formulation has resulted in relatively low density values that are 8%-12% less than theoretical. Thus, there is an increase in the amount of imperfections like cracks and air pockets that impact performance and present safety hazards contributing to casing over pressurization and failures. This discrepancy in propellant density has also encouraged erratic and unpredictable motor performance. Advancing from this, two additional sizes of ammonium perchlorate particles have been chosen in order to take the current mono-modal formulation to a tri-modal formulation. A tri-modal APCP formula will help reduce the amount of air pockets created during the

manufacturing process, close the gap between theoretical and actual propellant density, increase motor performance consistency, and reduce the risk of potential catastrophic failures.

The research objectives are as follow:

1. Given a fixed total percentage of ammonium perchlorate content, evaluate the effect of varying the amounts of ammonium perchlorate particle sizes within a tri-modal APCP formulation on performance consistency for future predictability.
2. Evaluate the effect that varying levels of ammonium perchlorate and aluminum percentages have on APCP performance consistency.
3. Evaluate the impact on motor performance consistency when total propellant length is divided into varying grain totals.

CHAPTER II.

BACKGROUND AND THEORY

2.1 Solid Rocket Motor Fundamentals

Rocket motors generally share a consistent set of key performance parameters. Typical performance measurables for solid rocket motors are thrust (F), specific impulse (I_{sp}), burn time (t_b), characteristic velocity (C^*), burn rate (r_b), chamber pressure (P_c), total Impulse (I), and thrust coefficient (C_f) [3]. These parameters are most directly related to aspects specific to each rocket and configuration, especially with regards to nozzle geometry and propellant composition. Thrust is a measure of the reaction force resulted from imparting momentum onto a mass and is one of the key inputs to several other performance parameters. Characteristic velocity is specific to the combustion of the propellant formulation, while chamber pressure and burn rate give implications on thrust magnitude and burn time duration. Total and specific impulse are measures of the energy exerted by the propellant itself, while thrust coefficient gives indication of a nozzle's effectiveness in accelerating exhaust gasses. When considering thrust produced by a rocket motor, it is important to consider the control volume in question. For the purposes of this analysis, a rocket engine mounted and secured to linear bearings with the forward closure butting directly against a button load cell is considered. Drawing the control volume so that only the solid rocket motor and load cell are included will result in the inclusion of propellant temperature, pressure, and mass flow properties within the casing. It is important to also note the inclusion pressure forces at the nozzle exit as depicted in Figure 4.

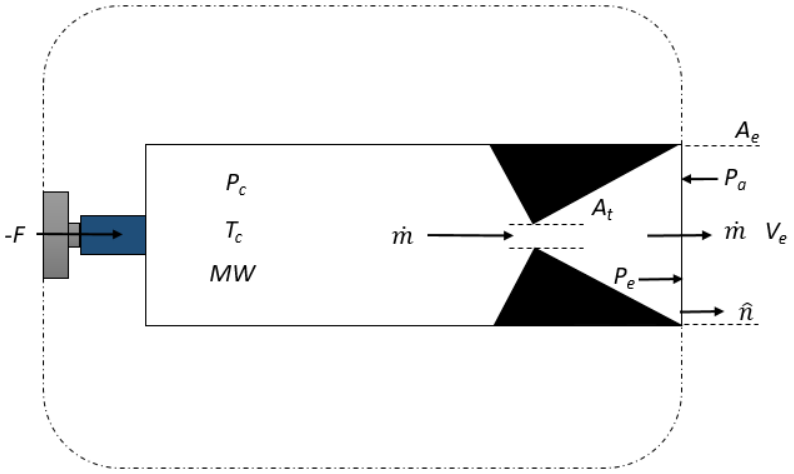

Figure 4: Control Volume to Determine Rocket Thrust on a Test Stand

Referring to Newton's second law of motion in Equation 1, and assuming a one dimensional and steady flow field along with observing that there are no influx properties coming into the control volume, the momentum equation can be simplified and ideally described as the sum of momentum and pressure forces exiting the control volume through Equation 3, using the expression for mass flow rate defined in Equation 2.

$$\frac{1}{g_c}\frac{\partial}{\partial t}\iiint_{cv}\vec{V}\,\rho\,d\forall + \frac{1}{g_c}\iint_{cs}\vec{V}\,\rho\left(\vec{V}\cdot\hat{n}\right)dA = \sum\vec{F} \tag{1}$$

$$\dot{m} = \frac{g*P_c*A_t}{C^*} \tag{2}$$

$$F = \frac{\dot{m}*V_e}{g_c} + (P_e - P_a)*A_e \tag{3}$$

The first term on the right side of Equation 3 is a measure of how much momentum the rocket motor is imparting, while the second term accounts for pressure thrust that is a result of nozzle performance. The momentum term will account for the majority of the thrust produced while the pressure term can be positive, negative, or zero depending on if the nozzle is under, over, or perfectly expanded. Perfect expansion results in ideal nozzle performance and indicates that the nozzle exit pressure is equal to ambient pressure. This results in the pressure terms within the

steady and one dimensional thrust equation to be equal to zero. Figure 5 serves as a visual representation for the different modes of nozzle performance.

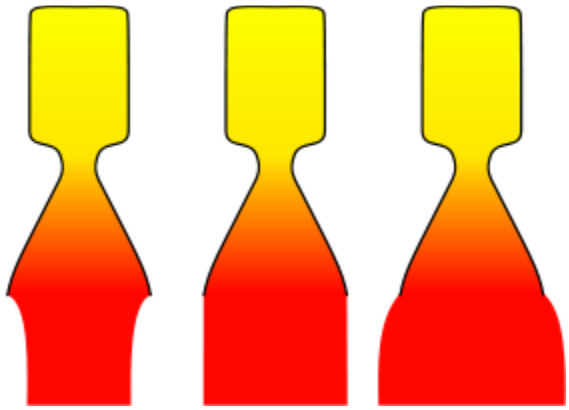

Figure 5: Over Expanded (Left,) Perfectly Expanded (Center), and Under Expanded (Right) Nozzles [4]

Specific impulse (I_{sp}) is a measure of a rocket's thrust per unit of propellant gas weight-flow exiting the nozzle. In the case of solid rocket motors, this can also be described as the ratio of total impulse to propellant mass consumed throughout the duration of its burn. It is in this area that traditionally solid rocket motors perform worse than other forms of chemical rocket propulsion as it requires a large amount of propellant weight in order to produce comparable amounts of thrust. This parameter is also helpful in assessing performance of a single formulation type as propellant mass may vary slightly, but the energy content per unit of mass should stay relatively constant. The equation for specific impulse can be observed in Equation 4 below.

$$I_{sp} = \frac{F}{\dot{w}} \tag{4}$$

Characteristic velocity (C^*) varies based on the propellant composition, as expressed in Equation 5, and is used to get a sense for the amount of energy available. Characteristic velocity can be expressed as a function of propellant chamber pressure, nozzle throat area, and mas flow rate or as a function of propellant chemical compositional characteristics that are specific to that particular propellant formulation.

$$C^* = \frac{P_c * A_t}{\dot{m}} = \sqrt{\frac{R_u * T_c}{\Upsilon * MW}} * [{}^{2}/_{\Upsilon + 1}]^{\frac{-(\Upsilon+1)}{2*(\Upsilon-1)}} \quad (5)$$

A rocket motor's burn rate (r_b) is a function of chamber pressure and a set of empirical constants known as the burn rate coefficient (a) and burn rate exponent (n) as shown in Equation 3. A motor's burn rate coefficient and exponent can be determined experimentally and is unique for each propellant composition. It is important to note that burn rate is not unit less and actually has Imperial units of $\frac{in*psi^n}{s}$, or $\frac{cm*MPa^n}{s}$ for SI units.

$$r_b = a * P_c^n \quad (6)$$

The burn time (t_b) of a motor is determined through use of the general thrust profile exhibited throughout the entirety of its burn. A motor's thrust profile will typically portray an initial rise, followed by some fort of sustained thrust output, and end with either a slow or quick deterioration in thrust produced. Within this study, burn time is characterized to start at the 75% maximum thrust value exhibited on the initial rise, and end at the 10% total maximum thrust value during thrust deterioration, as shown in Figure 6 below.

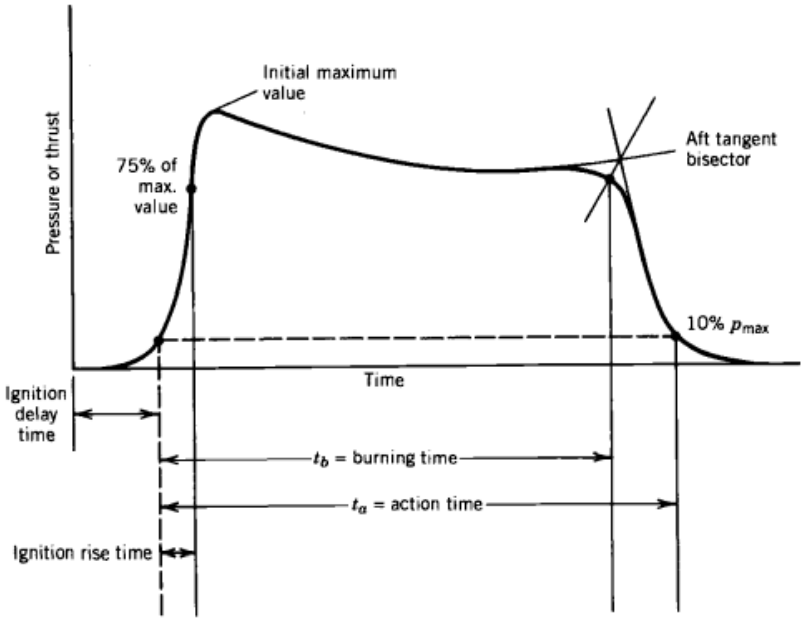

Figure 6: *Definition of Motor Burn Time [5]*

The chamber pressure (P_c) within the aluminum casing is a key parameter of interest because it determines how fast the propellant grains will burn. The higher the chamber pressure the faster a motor's burn rate will be. Chamber pressure is also important for safety purposes. Motor casings must be built with the intent of being able to contain the forces being exerted onto the casing from gasses being burned and accelerated through the nozzle. Assuming a fixed nozzle geometry, nearly constant pressure across the length of the propellant grains, and that mass flow through the nozzle varies minimally across the motor's burn time ($\dot{m}_{in} = \dot{m}_{out}$), instantaneous chamber pressure can be solved as shown in Equation 7.

$$P_c = \left[\frac{a * \rho_p * A_b * C^*}{g * A_t}\right]^{\frac{1}{(1-n)}} \tag{7}$$

From this, the propellant formulation will hold burn rate coefficient, burn rate exponent, propellant density, and characteristic velocity constant, leaving the profile of the motor's chamber pressure across its burn time to mirror the instantaneous total burning surface area. Total impulse is measured through taking the integral of thrust produced over the burn time of the rocket motor and is used to quantify the total amount of energy exerted by propellant. Simplification of this integral can be done if either thrust or specific impulse is assumed to be constant as shown in Equation 8.

$$I = \int_0^{t_b} F \, dt = F * t_b = I_{sp} * m_p \tag{8}$$

Finally, thrust coefficient is a dimensionless parameter used to indicate the amount of thrust produced relative to its chamber pressure and throat area as expressed in Equation 9. Thrust coefficient is maximized under the condition of perfect expansion, making it a good metric for measuring aspects related to nozzle performance.

$$C_f = \frac{F}{P_c * A_t} \tag{9}$$

2.2 Solid Rocket Motor Types

Chemical propulsion can encompass a wide range of rocket types and compositions, but at its core all chemical type propellants require an oxidizing agent and a fuel to facilitate the proper chemical reaction. Solid propellants are generally split into two major categories based upon the ingredients introduced and their resulting mixture. A double base propellant will molecularly combine fuel and oxidizer to form a new homogenous monopropellant substance. This is most commonly done by using nitrocellulose as a polymeric binder and a high energy liquid plasticizer, such as nitroglycerin, along with the introduction of some various other additives [6]. These propellants have, in the past, been mostly used in military missile applications, but are losing favorability due to their molecular instability [7]. Contrary to the homogeneity of a double base propellant, a composite propellant forms a heterogeneous mixture of solid fuel and oxidizer that is held together through a binder. There are a variety of different fuels and oxidizers used in composite propellants. Examples of some fuels include magnesium, zirconium, and beryllium while ammonium nitrate, potassium perchlorate, and sodium nitrate are some examples of oxidizers. The most popular fuel used is aluminum while the most common type of oxidizer is ammonium perchlorate. Binders include materials such as nitrate ester polyether (NEPE), glycidal azide polymer (GAP), and polybutadiene acrylonitrile (PBAN), but hydroxyl-terminated polybutadiene (HTPB) is especially used in a wide variety of applications today [3]. These three major ingredients are widely used together and makeup the foundations for APCP based solid motors.

2.3 APCP Composition

As mentioned, the key components to any solid propellant include an oxidizer, fuel, and binder. Along with these key components, there are several other ingredients that should be noted that could act as plasticizers, curing agents, and opacifiers that also serve as several other additive roles. [8]. The addition, subtraction or substitution of such ingredients will have large impacts on

motor performance. An easy way to observe how variations in composition affect motor performance is through looking at simulations. OpenMotor contains built-in solid propellants that can be modeled for given inputs of motor geometry. For example, when the grain geometries of a potassium nitrate/sorbitol propellant (KNSB) and an ammonium perchlorate composite propellant (APCP) are held exactly the same, performance expectations between the two will be significantly different. Even comparing between two propellants of generally the same compositions, there are notable differences in expected performance. To illustrate these differences, a small 38 mm (1.50 in) diameter motor was simulated in OpenMotor using KNSB and two different types APCP. The geometry consists of a 0.5 in BATES grain core and a size 22 Loki Research graphite nozzle [9]. See Appendix A.1 to view these simulations. It is easy to observe from these simulations that varying only propellant composition brings significant differences in parameters like burn time, chamber pressure, and thrust along with their profile shapes.

Different propellant materials can provide attributes like higher performance and long storability with the typical compromises such as moderate to high cost or non-environmentally friendly exhaust products. Various methods for solid composite propellant manufacturing can allow for easy and relatively fast production of motors, but overall composition, order of material introduction, and duration or timing of intermediate steps, such as propellant degassing, will cause variations in propellant properties that will affect motor performance repeatability and predictability. With so many variables affecting the performance of solid rocket motors, it is important to study the effect that variations of these variables have. In particular, a study of performance variations with respect to differing levels of oxidizer particle size, propellant composition, and propellant geometry should be had in order to quantify motor consistency relative to levels of key components and design choices within a motor's composition.

2.3.1 Oxidizer: Ammonium Perchlorate

Ammonium perchlorate stands out as the main ingredient of choice serving as the oxidizer for a composite solid motor. An APCP based formulation offers good performance at a moderate cost. Ammonium perchlorate offers higher values of specific impulse compared to other commonly used oxidizers while typical pricing can be found to be around $25 per pound dependent on particle sizing. It also has the advantage of having recently been removed from the list of items that are regulated under federal explosives laws by the Bureau of Alcohol, Tobacco, Firearms and Explosives (ATF) for particle sizes greater than 15 μm [10]. This indicates that individuals are no longer required to obtain a federal explosives license or permit in order to manufacture, import, purchase, distribute, transport, or receive APCP allowing for ammonium perchlorate based propellants to be easily attainable and widely accessible for experimental use. As mentioned earlier solid propellants are used in many high profile rocket and space exploration applications with ammonium perchlorate as the typical oxidizer of choice. Often times ammonium perchlorate can make-up 60-90% of the total percent weight for propellant formulations [11]. Ammonium perchlorate's ability to makeup such a large formulation percentage is due to its ability to act as both a fuel and an oxidizer, meaning that it is completely self-sufficient and does not require a separate ingredient to be added in order to serve as a fuel. Despite its wide usage, the decomposition mechanism of ammonium perchlorate is not very well understood. This in large part can be attributed to the oxidation states of the four elements that ammonium perchlorate's molecule is comprised of and their chemical reactions. However, with ammonium perchlorate being the main ingredient within APCP rocket motors, it is important to capture where the understanding of its thermal decomposition currently stands.

Ammonium perchlorate (NH_4CLO_4) is comprised of the elements Nitrogen (N), Hydrogen (H), Chlorine (CL), and Oxygen (O). When the oxidation states of these four elements are considered, over 1000 possible chemical reactions can occur for the decomposition of

ammonium perchlorate [12]. Additionally, other energetic materials used in propellants and explosives typically consist of only carbon, hydrogen, nitrogen, and oxygen while ammonium perchlorate includes the presence of chlorine, contributing to the complicated reaction chemistry. Lastly, ammonium perchlorate used in solid rocket propellants is 99.3-99.8% pure which could lead to the differing and occasional contradictory results for the decomposition and combustion characterization of ammonium perchlorate. Ammonium perchlorate impurity has been shown to especially affect burn rate characteristics, which is key in APCP performance consistency [12] [13].

The thermal decomposition process of ammonium perchlorate has been studied and several different mechanisms have been proposed. There are three different mechanisms that are typically discussed to describe the thermal decomposition for ammonium perchlorate, but their validity is still frequently debated. The three mechanisms include; the transfer of electron from an anion to cation, the proton transfer of cation to anion, or from the rupture of a chlorine-oxygen chemical bond [12, 14].

Electron Transfer from Anion to Cation [15]*:* Bircomshaw and Newman proposed an early version of the anion to cation mechanism and stated that it is instigated by a local electron transfer from a perchlorate to an ammonium ion:

$$ClO_4^- + NH_4^+ \rightarrow ClO_4^0 + NH_4^0 \quad (10)$$

With this being a local electron transfer between ions, there is a higher probability of this occurring and thus only interstices ammonium ions are suitable electron acceptors. The ammonium radical can now decompose into ammonia and a hydrogen atom after the reception of an electron:

$$NH_4^0 \rightarrow NH_3 + H \quad (11)$$

Local electron transfer over the anion sub-lattice between the perchlorate radical and ion occurs:

$$ClO_4^0 + ClO_4^- \rightarrow ClO_4^- + ClO_4^0 \quad (12)$$

Migration of the hydrogen atom over the lattice occurs and begins to interact with the perchlorate radical to form $HClO_4$ that can now begin to continue interacting with hydrogen.

$$HClO_4 + H \rightarrow H_2O + ClO_3 \quad (13)$$

Electrons are capable of then being trapped within the ClO_3 radical which transforms it into a ClO_3^- ion. ClO_4 radical and chlorite ion decompose and begin interacting with NH_4^+ ions. This decomposition results in several secondary products that includes water, chlorine, and nitrogen hemioxide. Arguments for this mechanism typically pointed towards ammonium perchlorate's thermal decomposition sensitivity to irradiation and oxides. However, arguments against indicate that the electron transfer mechanism cannot be sustained at low temperatures due to ammonium perchlorate being a dielectric. This means that for temperatures under 450 ^oC, the probability for the direct transfer of electrons is too low in order to sustain decomposition per the "forbidden gap" in the energy-band theory.

Proton Transfer from Cation to Anion [12, 16]*:* The theory for this mechanism was supported by the similar values for activation energy and identical product composition for thermal decomposition and sublimation. Additionally, ammonia vapor reaction inhibition and the acceleration of perchloric acid in the ammonia vapor are considered to confirm the appropriateness of the proton transfer mechanism. A version of the proton mechanism for the thermal decomposition of ammonium perchlorate was proposed by Jacobs et al.:

Initially a pair of ions exist in the perchlorate ammonium lattice. Decomposition is then provoked through proton transfer from the NH_4^+ cation to the ClO_4^- anion binding the molecules together forming a molecular complex, this is then proceeded by decomposition of the molecular complex

into ammonia and perchloric acid. From here the ammonia and perchloric molecules will either react in the adsorbed layer on the perchlorate surface or release and vaporize to begin interacting in the gas phase. At temperatures below 350 ^{o}C the surface reaction proceeds faster than sublimation, while at temperatures above 350 ^{o}C the opposite occurs. It is assumed that for the reaction occurring in the adsorbed layer, perchloric acid is desorbed faster than ammonia leading to the incomplete oxidization of ammonia. This leads to an ammonia saturated surface bringing the reaction to an end and results in the incomplete transformation of perchlorate.

$NH_4^+ + ClO_4^- = NH_3$ (a) + $HClO_4$ (a) = NH_3 (g) + $HClO_4$ (g)

This model has been criticized for its simplicity and inability to explain certain physical and thermal properties of the reaction that still remain unclear. This includes the addition of ammonia having an effect at high pressures and stops having an effect at low pressures, despite its partial pressure being several times higher than equilibrium. Also, it is perchloric acid and not ammonia that is accumulated in perchlorate. Corrections to this model have been proposed that advance understanding of the thermal decomposition of ammonium perchlorate, but additional investigations are still required.

Rupture of a Chlorine-Oxygen Chemical Bond [12, 15]*:* This mechanism is associated with the investigation of ammonium perchlorate thermal decomposition above 350 ^{o}C. It is at these higher temperatures where ammonium perchlorate decomposition occurs within the combustion of solid composite propellants. Bircomshaw and Newman determined that the activation energy of ammonium perchlorate was on the same order as potassium perchlorate for thermal decomposition, about 293 kJ/mol. This allowed for the conclusion that ammonium perchlorate decomposes under similar conditions as potassium perchlorate with the rupture of chlorine-oxygen bond being the primary stage. This mechanism shows that high temperature thermal decomposition begins through the same manner as the proton transfer mechanism, a proton

transfers from an ammonium ion to a perchlorate ion. Secondary chemical reactions occur on the ammonium perchlorate surface or in the gas phase just above the surface as a result of the interactions between the thermal decomposition products of perchloric acid and ammonia. The mechanisms of these secondary reactions will change as temperature and pressure is changed. It is at this point where criticism of this mechanism begins as the ammonium perchlorate thermal decomposition activation energy equaled 88 kJ/mol, which proved to be less than the heat of sublimation, that being 125 kJ/mol. Thus, the heat required to transform ammonium perchlorate from a solid to a gas state is not met through this mechanism. When posed with this discrepancy, many choose to assume that quasi-equilibrium has been established on the surface of ammonium perchlorate between the disassociation products and the perchlorate which results in the activation energy being equal to just half of the heat of sublimation. Another way to deal with the low activation energy is to consider Volmer's model of stepwise evaporation [17]. It accepts that the probability of molecular transition from solid to gas phase through a single step is low and instead proposes the rupture of bonds that transitions the ammonium perchlorate crystals from a highly bound state to a lesser bound state. Attempts have been made to characterize the states that ammonium perchlorate goes through during thermal decompositions, which have resulted in the structure of a molecular complex being proposed that precedes ammonia and perchloric acid molecules being removed from the ammonium perchlorate crystal.

While the proton mechanism has become widely accepted by researchers as being the most likely theory for explaining the initial stages of thermal decomposition for ammonium perchlorate, arguments for the electron transfer mechanism still exist. Thus, this lack of consensus and ongoing area of discovery contributes to the amount of uncertainty that comes when using ammonium perchlorate as an oxidizer for solid composite propellants.

2.3.2 Fuel: Aluminum

A solid fuel is desired within solid rocket propellants as it is key in absorbing the heat produced from combustion in order to vaporize and facilitate combustion reactions. Aluminum is the most common choice of fuel used in composite propellants and can typically make-up anywhere between 2%-21% of a formulation [3]. The introduction of a fuel in the form of metal aluminum particulates has been determined to increase specific impulse and improve combustion stability. Aluminum is also able to be stored for long periods of time and is known to be relatively low cost.

Upon ignition of the propellant containing oxidizer and aluminum fuel, the metal particles will melt, accumulate together, and combust through an aluminum oxidation reaction. Aluminum releases a high amount of energy during this combustion reaction and results in a great amount of gas expansion within the combustion chamber. Aluminum's ability to rapidly expand combustion gasses results in its ability to increase specific impulse, while the agglomeration of small molten aluminum particulates is the main cause for dampening of combustion instabilities. This has resulted in several studies to be conducted on how aluminum affects the performance of solid motors. These studies primarily focus on the size of the aluminum particles themselves and will typically compare the use of micro-aluminum particles against nano-aluminum particles. Meda et al. and Galfetti et al. compared such sizes of aluminum particles and noted their effects on propellant characteristics such as ignition time, temperature, and burn rate [18, 19]. It was shown that the use of nano-aluminum particles between 0.1 μm to 0.2 μm had the ability to reduce ignition time and enhance burn rate linearization, while also increasing burn rate. For particles sizes above 1 μm the burn rate remained unaffected. These characteristics are a product of the increased reactivity of the aluminum powder due to its smaller size. The smaller aluminum sizes intensify the energy released as a result of the increase in specific surface size, i.e. surface area per unit mass, of the particles and by particle oxidation occurring closer to the burning

surface of the propellant [19, 20]. These smaller particles also help increase propellant density, specific impulse, and combustion efficiency at the expense of higher costs, issues with safety, and poor mechanical properties. Additionally, performance parameters can also decrease with the use of smaller particles due to their tendency to clump together during manufacturing. This also is observed during the burning of motors and can create slag buildup near the nozzle throat, making it important to coat the aluminum particles with a protective layer or selecting a binder that can help reduce the amount of aluminum that goes unburned [19, 20, 21].

2.3.3 Binder: HTPB

A binder's main function is to give structure to the components of the propellant formulation. HTPB is a polyurethane based binder and pairs well with the choice of an ammonium perchlorate oxidizer as it provides the highest specific impulse [22]. HTPB was specifically created to be used as a propellant binder. High density and tensile strength give good structural properties while HTPB also provides a fast burning rate, high combustion energy, and allows for higher solids fractions as it only needs to make-up about 10% of the total propellant weight [23]. All of these qualities contribute to HTPB being the most widely used binder for large scale rockets, specifically booster stages. A binder's ability to give desirable physical and mechanical characteristics is primarily dictated by its network. The most important parameter of a binder is known as crosslink density (CLD), which is defined as the moles of elastically effective network chains per unit of volume [23]. Studies such as in the one conducted by Sekkar and Raunija have worked to be able to predict solid propellant physical properties through the modeling of urethane networks in order to derive CLD's. Their work has shown that higher CLD values correspond to an increase in propellant grain tensile strength, regardless of the solid concertation within the formulation when using HTPB-based urethane networks, as shown in Figure 7.

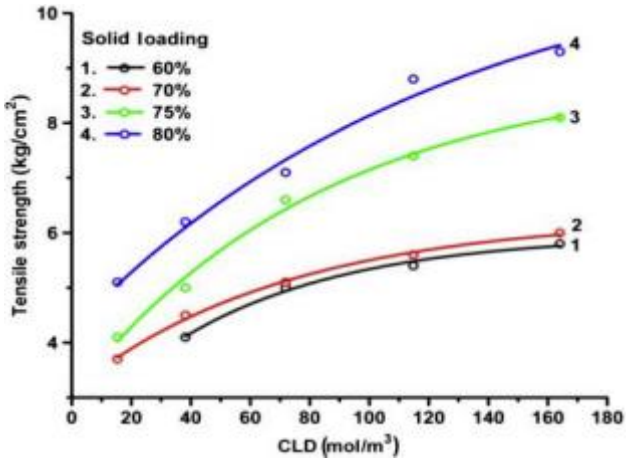

Figure 7: Calculated CLD vs. Tensile Strength for Solid Propellant grains of various Solid's Loading [23]

2.3.4 Other Additives

Several other ingredients that serve additional roles besides as an oxidizer, fuel, or binder can be added to a solid composite propellant's formulation. These typically will include a burn rate modifier or catalyst, plasticizer, curing agent, and other filler bonding agents. Burn rate modifiers are typically very fine metals that are added in small amounts in order to speed up or slow down the burning rate of the propellant. The catalyst of choice in this study is copper chromite which is known to accelerate the thermal decomposition rate of ammonium perchlorate [12]. Copper chromite also serves the advantage of acting as an opacifier that darkens the propellant to reduce the amount of radiation present during a motor's burn that can cause heating in places other than on the burning surface of the propellant. Catalysts that increase propellant burning rate are typically used in order to meet thrust and time project requirements along with allowing for a variety of desired grain designs [24]. Other burn rate modifiers include ingredients such as lithium fluoride which is used to decrease propellant burning rate. Plasticizers are relatively low-viscosity liquids that enhance thermal energy and improve the process-ability of the propellant aiding in the ability to manufacture solid motors. A plasticizer will also be added to improve propellant strain capabilities and reduce the glass transition temperature. Dioctyl adipate (DOA) has been chosen as the plasticizer for the formulation used in this study, but other commonly used plasticizers include nitroglycerine (NG), glicidyl azide polymer (GAP), and

diethyl phthalate (DEP) [24]. Some form of curative is necessary in order to promote crosslinking to hold the ingredients suspended within the binder in place. The curative promotes the formation and interlocking of longer chains with higher molecular mass to be formed that solidify and harden the binder. Since HTPB is being used as the binder of choice, an isocyanate-based curative is required to enable crosslinking between the hydroxyl groups in the polymer. Thus, methylene diphenyl diisocyanate (MDI) is the curing agent of choice for this study [3]. Additional minor additives to be used include tepanol and castor oil. These are used as filler-bonding agents added in low concentrations that promote physical and chemical interaction between oxidizer and binder ingredients. A reduction in mechanical and ballistic properties can be the result of humidity corrosion on the oxidizer surface due to poor interaction between oxidizer and binder, making the use of filler-bonding agents popular in order to increase the strength and storability of the propellant [25]. Additionally, high propellant mechanical properties are essential for applications that experience a large amount of acceleration, to prevent grain fracture due to propellant structural instability

2.3.5 APCP Pros and Cons

APCP-based rocketry, and solid rocket motors in general, are still one of the most attractive options as a source of chemical propulsion because they have the advantage of simplicity without the huge compromise in performance [3]. Solid motors offer the highest amount of volumetric impulse, indicating they are great for applications where the amount of space available is limited. Solid forms of chemical propulsion also have the advantage of being quite simple in both motor design and manufacturability, while also having the ability to be stored in case usage is not immediate. The tradeoff for this simplicity being that a large amount of weight is needed in order to produce comparable magnitudes of thrust and the inability to easily incorporate throttling. This usually indicates that, once ignited, solid motors can only burn to completion without being turned off or tailored throughout the duration of a motor's burn which

is a key advantage when implementing a liquid or hybrid system instead. Additionally, the large amount of weight required results in low values of specific impulse compared to other forms of rocket propulsion as illustrated below in Figure 8.

Fuel/oxidizer	I_{sp}, s
Solid propellant	250
Liquid O_2: kerosene (RP)	310
Liquid O_2: H_2	410
Nuclear fuel: H_2 propellant	840

Figure 8: Ranges for Specific Impulse for typical rocket engines [5]

Other disadvantages are related to the environmental impact of APCP motors. The exhaust products are known to contain hydrogen chloride, chlorine, and ammonia particles that result from combustions of ammonium perchlorate based formulations. Hydrogen chloride and chlorine emissions are large factors contributing to catalytic ozone depletion while particles of ammonia serve as condensation platforms within the stratosphere and mesosphere that also facilitate ozone depleting. However, the impacts of APCP specific emissions globally are largely considered to be negligible despite uncertainties in the ammonium perchlorate combustion process, and the lack of detailed emissions data [1, 26, 27]. While the exhaust products of ammonium perchlorate are known to being environmentally harmful, substitution of ammonium perchlorate for another oxidizer, such as ammonium nitrate, will lead to cleaner exhaust products with a decrease in propellant performance [3].

2.4 Solid Propellant Manufacturing

2.4.1 General Propellant Formation Process

Solid rocket motors must be manufactured with the idea that its propellant must be able to maintain structural integrity throughout any handling or storage that my take place prior to ignition, as well as being able to endure the loads and vibrations during launch. Once manufactured, mechanical or ballistic performance inspection of these grains cannot be done

without compromising the integrity of the propellant itself, therefore particular attention must be made towards the procedures of mixing and casting solid propellant grains. The two main approaches to propellant manufacturing are either batch or continuous processing. Batch processing usually involves either a conventional or industrial mixer in which propellant is mixed and then casted into a motor that may be a product of one or more separate batches. Continuous processing typically will require a screw-type machine that will constantly feed propellant into motor casings in an assembly line fashion. Batch processing is the typical method of choice as most applications do not require the amount of propellant volume to make continuous processing procedures attractive [3]. Once the desired processing type has been selected, ingredients are then weighed out on a percent weight basis. Initially fuel and all wet ingredients, except for the curative, should be combined in order to bring the formulation to a state of "fuel premix". Once the premixed fuel blend has been created, the oxidizer can now be introduced gradually. When multiple sizes of oxidizer particles are used, the larger particles should be introduced first to promote mixing due to the reduced friction associated with their smaller surface area. Once all ingredients incorporated, the curative can be added and mixed into the formulation while being careful to keep mixing to a relative minimum as the formulation will begin to solidify with time. After effective incorporation of curative has taken place, the propellant mixture can then be placed into a casting tube where the remainder of the curation process will take place [3]. Grain geometry is important to consider prior to casting as typically that will dictate the shape and size of the coring rod or mandrel that is used. The coring rod will need to be properly positioned inside of the casting tube prior to propellant packing so that propellant can be poured or placed around the rod, leaving the desired exposed surface shape within the casted grains after rod removal.

2.4.2 Propellant Geometry

The geometry of propellant grains themselves have a big impact on the amount of thrust expected from a solid motor and how that thrust will be delivered. Initial grain geometry dictates the amount of surface area being burned at a given instant. As previously observed in Equation 7, motor chamber pressure increases with exposed burning surface area. Now referring back to Equation 3 using Equation 2, we conclude that chamber pressure is directly proportional to thrust produced. Thus, an increase in the exposed burning surface area will also result in an increase in motor instantaneous thrust produced. As a motor progresses through the duration of its burn, the exposed burning surface area of the grain may increase, decrease, or stay the same. This indicates that the initial grain geometry plays a big role in how much thrust is being produced at a given point throughout a motor's burn, and will shape the overall burn profile. Typical burn profiles exhibit progressive, regressive, or neutral behaviors. Progressive profiles increase in thrust as burn time progresses, a regressive behavior results in a decrease in thrust over burn time, while a neutral profile will keep thrust nearly constant over the course of a motor's burn. While a neutral burn profile is desirable among most applications, it typically requires a relatively complex initial core geometry in order to keep the burning surface area constant with respect to burn time. This can make it difficult to create and remove whatever form of structure is being used to form the geometry of the grains. For this reason, a tubular grain core is a popular grain geometry of choice, as it is a shape that can be easily acquired and removed from the casted propellant. Additionally, while a tubular geometry is typically associated with a progressive burn profile, studies have enabled increased burn profile neutrality such as in what was observed in Noaman at al. [28]. Observation of several various core geometries and their typical burn profiles can be observed in Figure 9 below.

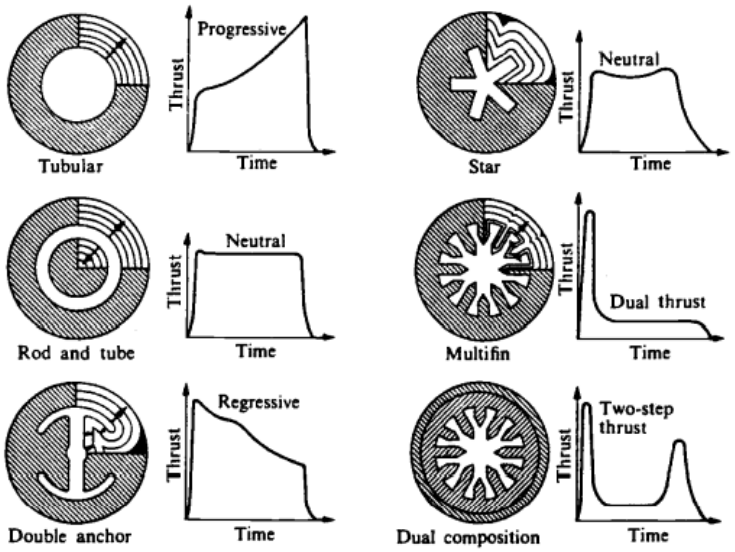

Figure 9: Grain Geometry Design and Typical Burn Profiles [5]

2.5 Previous Works on Tri-Modal APCP Propellants

Typically, multiple particle sizes of ammonium perchlorate are mixed in order to increase propellant density, decrease viscosity, and adjust burn rate. As mentioned before, solid propellant formulations with high density and specific impulse are desirable. Several works documenting the affects that varying ammonium perchlorate particles sizes in multi-modal compositions exist and will focus on analyzing propellant burn rate, viscosity, rheological, and mechanical properties. Studies have concluded that while using only two particles sizes of ammonium perchlorate is rather simple and easy to design, these propellant formulations become difficult to cast beyond concentrations above about 70% ammonium perchlorate total weight, or a solid loading above 86% due to the sharp increase in viscosity [11, 29]. This manufacturing cap on ammonium perchlorate concentration in turn limits the amount of burn rate adjustment possible [30, 31]. Thus, three different types of ammonium perchlorate particle sizes are usually implemented to improve viscosity allowing for easier propellant casting and increased potential burn rate modification.

Park et al. analyzed propellant properties of tri-modal ammonium perchlorate and HTPB formulation using particle sizes of 400, 200, and 6 μm (AP-400, AP-200, and AP-6 respectively)

[11]. When the percent weight content of AP-6 was held constant at 20% and values of AP-400 and AP-200 were varied, significant changes in viscosity were not observed. Lower viscosities were the result of an increase in AP-400 content within the approximate range of 30% to 45% weight. When AP-400 and AP-200 concentrations were held at a 1:1 and AP-6 content was varied, lower values for propellant viscosity were achieved for AP-6 concentrations between approximately 15% and 35% as observed in Figure 10 below.

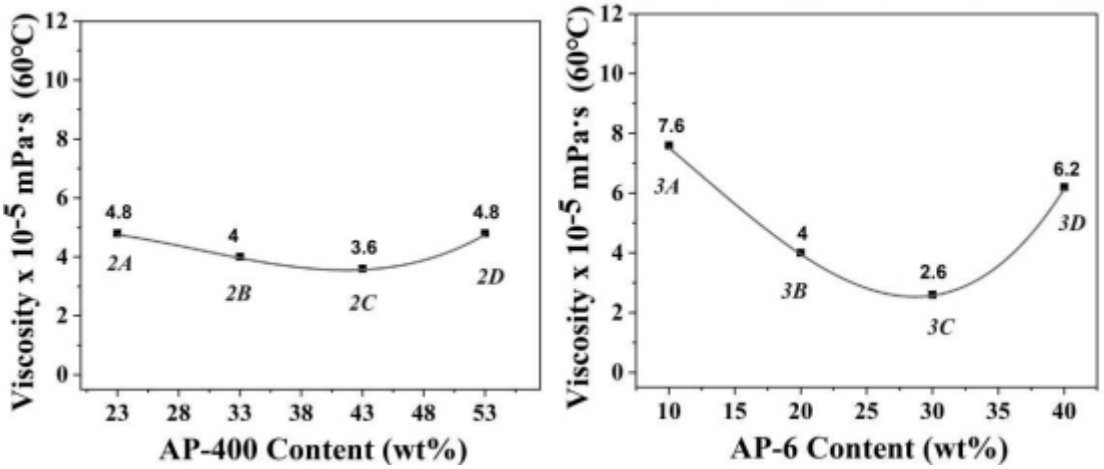

Figure 10: APCP Tri-Modal Propellant Viscosity with varying AP Concentrations [11]

Babu et al. experienced similar results while using a formulation comprised of coarse, fine, and ultrafine ammonium perchlorate particles, those being AP-340, AP-40, and Ap-5 [29]. Lower viscosities were generally achieved when AP-5 content was increased, and maximum tensile strength was achieved when viscosity was lowest at total ammonium perchlorate ratios being 67% AP-340, 24% AP-40, and 9% AP-5.

Burn rate has been extensively observed as a function of ammonium perchlorate particle sizes and concentrations. It is important to note that the burn rate of solid rocket propellants is typically correlated through the power-law approximation observed in Equation 6. A burn rate study on ammonium perchlorate particle size and concentration influence in mon-modal formulations was conducted by Thomas et. al. for sizes ranging from 20 to 500 μm and for concentrations ranging between 70% and 80% weight [32]. Results showed that burn rate

increased with ammonium perchlorate concentration and a decrease in the particle size, with burn rate being much more sensitive to particle size rather than to overall ammonium perchlorate concentration. Rodić and Bajlovski gathered burn rates and mechanical properties on varying tri-modal ammonium perchlorate propellant particle sizes of 200, 400, and 80 μm while keeping the total solid content constant throughout [33]. A high fraction of AP-400 slowed burn rates while higher burn rates were observed when fractions of AP-200 and AP-80 were equal. Fractions of ammonium perchlorate that were high in AP-200 and AP-400 exhibited lower tensile strengths due to the decrease in surface area contact between the binder and oxidizer. The opposite was observed for strain properties as higher AP-400 concentrations gave enhanced values. The results discussed in Park et al. were similar to the tri-modal burn rate properties observed in Rodić and Bajlovski [11, 33]. When only coarse particles of AP-400 and AP-200 were varied there was no significant increase or decrease in burn rate. In cases where AP-6 concentration was varied, an increase in burn rate was observed with an increase in AP-6 content. Additionally, a reduction in burn rate was observed when the concentration of ammonium perchlorate was reduced for an ammonium perchlorate and HTPB based propellant. These findings are also supported in Babu et al. as an increase in ultrafine AP-5 content increased propellant burning rate in an ammonium perchlorate, aluminum, and HTPB composition [29].

The predominant nature of studies concerning tri-modal ammonium perchlorate variations have been focused on propellant mechanical strength and strain properties and archiving or analyzing burn rate characteristics as a function of particle size concentration. There is a lack of research into the affects that particle size variations could have on performance consistency and repeatability. With burn rate characterization being largely statistical and typically being the primary focus of previous works related to propellant performance, it seems fitting that a stochastic approach to characterization of other APCP performance parameters with respect to different particle sizes and propellant geometry be had towards analyzing their effects

on motor consistency. Thus, the purpose of this study is to evaluate several tri-modal ammonium perchlorate formulations and motor configurations in order to observe the nature with which performance parameters may vary.

2.6 Theory of Analysis

This study focuses on five different rocket performance parameters and their statistical variations. These parameters are peak thrust, average thrust, burn time, total impulse, and specific impulse. Three variations in ammonium perchlorate particle size concentration, two different grain geometry lengths, and three different total concentrations of ammonium perchlorate were chosen in order to evaluate performance variations. Initially a total ammonium perchlorate and aluminum concentration of 75.80% and 5.02% weight, respectively, will be held constant for primary testing of ammonium perchlorate particle size variation. Particle sizes equaling 400 µm, 200 µm, and 90 µm will first contribute 1/3rd of the ammonium perchlorate total content and approximately 25.27% of the formulation total weight. In applying results mentioned above from Rodić and Bajlovski and Park et al., it is apparent that 200 µm variances do little to alter motor burn characteristics [11, 33]. Therefore, the AP-200 concentration will be held constant throughout, while increasing and decreasing AP-400 and AP-90 concentrations will be studied. Thus, after motors with an even distribution of ammonium perchlorate particles have been tested, formulations with a 10% weight increase in AP-400 content and a 10% weight decrease in AP-90 content will be evaluated. Subsequently, formulations with a 10% weight increase in AP-90 content and a 10% weight decrease in AP-400 content will follow. All three varying particle size formulations will be evaluated in 2 and 3 grain configurations to evaluate performance consistency with respect to motor geometry. After observing geometry and particle size affects, one of the tested geometries and average particle sizes was chosen for further evaluation, based on a combination of motor performance and propellant physical properties. The chosen average particle size and propellant geometry was applied to a study where the aluminum content is both

doubled and reduced to zero in order to observe variation affects with regards to aluminum content. All tests will be conducted on a 54 mm (2.13 in) diameter motor with a total propellant length equal to 6.68 in. Thrust will be recorded as a function of time for all tests.

CHAPTER III

EXPERIMENTAL METHODOLOGY

3.1 APCP Storage

The facility in which this study was performed is the Oklahoma State University Richmond Hill Research Laboratory. All ingredients and materials for motor fabrication, testing, and storage are located within the facility. A mobile ground test rig is utilized and allows for convenient storage during periods when motor testing is not occurring, while also providing a quick way for testing setup. All rocket motor related items are kept in a limited access and secure room within the facility that prevents unauthorized personnel to be in contact with items related to APCP motor fabrication and testing.

All motor ingredients are stored in explosives, flammables, and corrosives cabinets with each ingredient being designated to its proper storage cabinet as per their safety data sheets, with each ingredient's storage designation and hazard being:

- **Flammables Cabinet:**
    - Aluminum Powder (325 mesh)
    - Copper Chromite
    - Hydroxyl Terminated Polybutadiene Resin (HTPB)
- **Corrosives Cabinet:**
    - Dioctyl Adipate (DOA)
    - Tepanol

- Methylene diphenyl diisocyanate (MDI Curative)
- Castor Oil

- **Explosives Cabinet:**
  - Ammonium Perchlorate

3.2 APCP Motor Manufacturing

All mixing is done through the use of a KitchenAid® 4.5-quart tilt-head stand mixer. Mixing is conducted at low speeds to prevent airborne particulates from the various powders used in motor manufacturing. Mixing is limited to small propellant batches that fit within the standard 4.5-quart mixing bowl as per recommendations from the fire marshal. Due to favorable manufacturing, a BATES grain geometry was chosen.

3.3.1 APCP Mixing Procedures

Under the guidance for multi-modal oxidizer incorporation, coarser particles of ammonium perchlorate are added first with the finest particle size being added last to promote effective mixing [3]. Procedures for tri-modal APCP mixing are as follows:

1. Weigh ingredients to appropriate desired propellant ratios (ammonium perchlorate, aluminum powder, binder, and catalysts).
2. Add fuel, binder, and copper chromite together into mixing bowl, make sure that no airborne dust is created when adding metal powders.
3. Mix fuel, binder, and catalyst within bowl using KitchenAid® mixer at a speed setting equal to 1. (10 minutes)
4. Add and mix DOA, tepanol, and castor oil within mixing bowl at a speed setting equal to 2. (10 minutes)
5. Place mixing bowl into vacuum chamber and degas fuel premix binder mixture. Figure 11 provides visualization of this configuration. (60 minutes)

6. Remove bowl from vacuum chamber and slowly add 2/3rd of total amount of 200 µm oxidizer powder into mixture making sure that no airborne dust is created when adding powder to mixing bowl.
7. Mix oxidizer propellant mixture incrementally adding more oxidizer powder into bowl at speed setting equal to either 3 or 4. (10 minutes)
8. Repeat Steps 6 and 7 for 400 µm oxidizer.
9. Repeat Steps 6 and 7 for 90 µm oxidizer.
10. Place mixing bowl, with now all oxidizer added to propellant mixture, back into vacuum chamber for degassing. (60 minutes)
11. Remove bowl from vacuum chamber and add curative to total propellant mixture.
12. Mix curative into total propellant mixture. (10 minutes)
13. Once mixing is complete, place ingredients back in their respective cabinets and proceed to casting procedures.

Figure 11: *Propellant Degassing Chamber Configuration*

3.3.2 APCP Casting Procedures

Procedures for APCP casting are as follows:

1. Spray Aluminum casting caps and coring rod with a urethane mold release spray.
2. Place aluminum casting cap on one end of the casting tube before placing mixture into casting tube.

3. Position coring rod within the slot of the casting tube cap.
4. Position the casting tube with the coring rod upright on a level surface
5. Place/pour (depending on mixture consistency) propellant mixture into multiple spots within the rocket motor casting tube ensuring that the coring rod stays centered within the casting tube
6. Once a small amount of propellant has been added, diligently pack down the propellant into the casting tube using a dowel rod to tap the surface of the propellant repeatedly.
7. Continue to repeat Steps 5 and 6 until the desired amount of propellant has been placed and packed into the casting tube.
8. Close the other end of the casting tube with the remaining aluminum cap, ensuring the coring rod is aligned with the center of the casting tube as depicted in Figure 12.
9. Place the motor casting tube with the propellant mixture and coring rod upright in the wooden casting stand located in the explosives cabinet. Use tie down straps to apply light pressure to the top casting cap to maximize potential propellant density.
10. Allow propellant to cure within the explosives cabinet ensuring propellant has fully solidified. (24 hours)
11. Once the propellant is cured, remove the coring rod and casting caps from the casting tube and visually inspect the grain for any damages resulting from removal of the coring rod.
12. Weigh the propellant using a scale to record the weight after the casting process has concluded.
13. Use calipers to measure the dimensions of the grain in order to calculate propellant volume.
14. Use the weight and the volume of the grain to compute propellant density for comparison with the theoretical propellant density value. Propellant density must be

greater than or equal to 90% of the theoretical propellant density for a grain to be deemed acceptable.

Figure 12: *Casting of 54 mm Motor with Aluminum Casting Caps and Coring Rod*

3.3 APCP Motor Testing

3.3.1 Solid Propellant Test Preparation

Once propellant casting procedures have been followed and curation of propellant grains has concluded, removal of the coring rod can be done. The casted propellant is slid down the length of the coring rod, leaving a smooth cylindrical tube like structured mold within the propellant. Once removed, the propellant is then cut into to desired grain lengths through the use of a guided adjustable Mitre Saw, as pictured in Figure 13 below.

Figure 13: Adjustable Mitre Saw for Cutting Propellant Grains

Once grains have been cut to length, each grain face is lightly sanded, inserted into a correctly sized liner, and tested for adequate fitment within a motor casing. Once fitment of grains has been checked, each grain length and weight is recorded into a spreadsheet calculating grain density and comparing it to the theoretical propellant formulation density. Figure 14 and Figure 15 show examples of grain fit checking and comparison of propellant actual to theoretical density.

Figure 14: Liner, Propellant Grain, and Casing Fit Checking

54mm Motor 3-12 Test 2.3a				
	Grain 1	Grain 2	Grain 3	Total Motor
Length (in)	2.24	2.27	2.24	6.74
Mass (grams)	135.19	135.60	133.32	404.11
Volume (in3)	4.98	5.04	4.97	
Density (gr/in3)	27.17	26.90	26.83	
Density (lb/in3)	0.0599	0.0593	0.0591	0.0594
% Diff	0.06%	0.90%	1.20%	0.72%

Figure 15: *Propellant Grain Density Calculation and Comparison Example*

The high powered solid rocket motors discussed in this study are tested through the use of an aluminum outer casing and snap ring configuration. Also a converging diverging nozzle, nozzle washer, casting tube, casing liner, and forward closure are nested within the aluminum casing helping to secure the propellant and to prevent damage to the inner walls of the casing. Motor and casing configuration can be observed in Figure 16. Note that for motors tested in this study, a forward closure replaces what is referred to as a “plug” in the figure below.

Component Number	Component Name
1	Snap-Ring(s)
2	O-Ring(s)
3	Nozzle
4	Plug
5	Motor Casing
6	Casting Tube
7	Grain

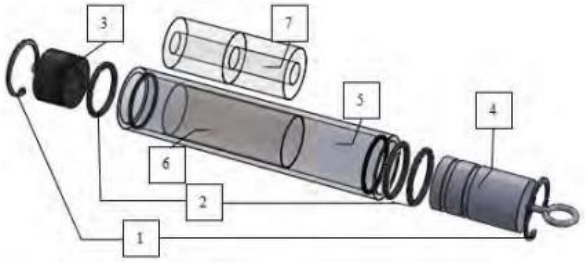

Figure 16: *General Motor Casing Configuration [2]*

Initially, motor assembly begins by inserting propellant grains into an appropriately sized liner. The outer surface of the liner containing the grains is coated with a thin layer of silicone grease. O-rings are then greased and placed within the proper grooves of the nozzle and forward closure. One end of the greased liner is then pressed onto the converging side of the graphite nozzle. The nozzle and liner, now housing the propellant grains, can now be slid into an aluminum casing making sure that the nozzle diverging section is facing the aft end of the casing when fully installed. A nozzle washer is then placed on the exit face of the nozzle, and the forward closure is slid into the casing through the forward side with the flat surface being flush to the faces of the propellant grains. Snap rings are then placed into the snap ring grooves on forward and aft sides of the casing.

3.3.2 Test Stand Configuration and Instrumentation

All motors were tested on mobile ground test stand. The motor is secured on linear bearings while the load cell has capable mounting points for motors with diameters ranging between 38 mm and 98 mm (1.5 in and 4 in) diameters. A power supply is mounted to the underside of the steel table top, providing power to an electric relay board in order to remotely ignite each motor. Ignition is controlled using a LabVIEW VI that is tailored to prevent

unintentional ignition. A thrust stand schematic and illustration can be viewed in Figure 17. The interface controlling ignition is viewed in Figure 18 [34, 35].

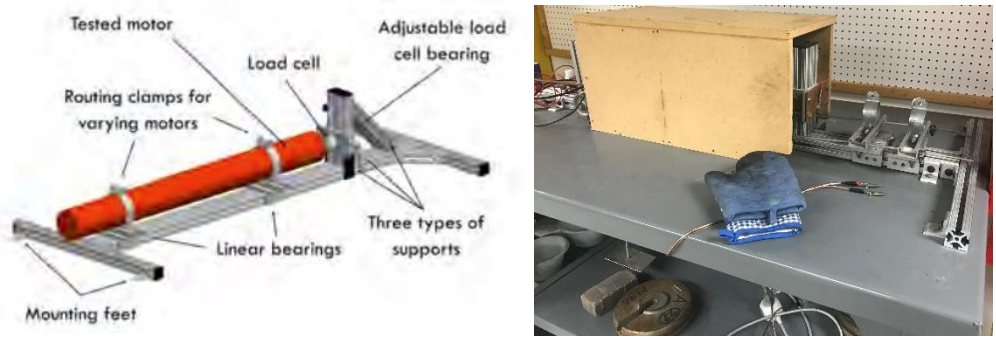

Figure 17: *Thrust Stand Overall Configuration [2]*

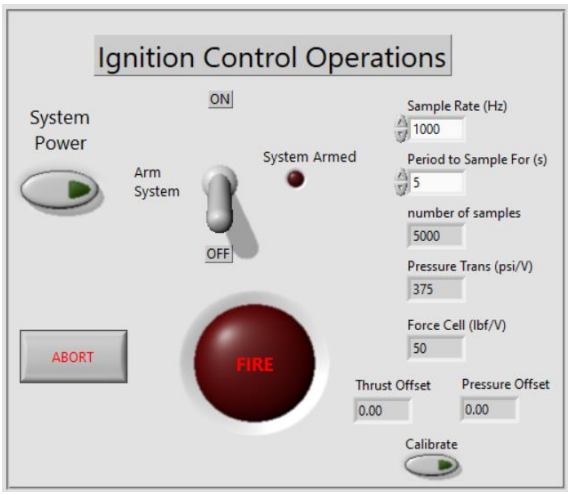

Figure 18: *LabVIEW Ignition Interface*

In order to record thrust measurements, a load button load cell rated for 2000 lbf (accuracy of ± 0.05% rated output) is mounted onto a forward facing fixed steel plate on the front end of the thrust stand [36]. This load cell includes software from SENSIT that is used in order to convert recorded samples into numerical values that are automatically exported into a Microsoft Excel spread sheet for further data reduction. It is within the SENSIT software that the load cell can be tarred and calibrated. Additionally, SENSIT offers features such as the ability to edit sample rate and observe live force measurements.

3.3.3 APCP Motor Testing Procedures

All testing is conducted behind the north loading dock at the Richmond Hill Research Laboratory. The testing environment allows for compliance with recommended safety precautions regarding standoff distances, hearing protection, and accessible fire extinguishers. National Association of Rocketry high powered launch safe standoff distances can be observed in Table 2 [37]. The preliminary test matrices for motors that were manufactured and tested is displayed in Appendix A.2 while final test matrices can be viewed in Table 4. Testing procedures for motor testing are as follows:

1. Use routing clamps found on thrust stand to secure rocket motor. Be sure to wrap the motor casing with slivers of grip shelf liner at the clamp locations to protect the outer casing and ensure the motor is secure gripped by the routing clamps.
2. Move the gripped motor assembly along the bearings until the forward end of the motor is in contact with the load cell.
3. Plug in the thrust stand power supply.
4. Plug thrust stand USB into laptop containing the LabVIEW test stand virtual instrument file, plug the load cell USB into the laptop containing an installed version of SENSIT test and measurement software.
5. Strip leads of motor igniter and attach them to thrust stand alligator clips. Be sure to touch alligator clips together before connecting igniter leads to ensure that no voltage is being sent through the igniter during installation.
6. Take installed igniter and insert it into the motor through the nozzle opening until igniter is seated against the forward closure and forward-most propellant grain.
7. Apply 20 lbf pre-load to thrust stand load cell.
8. Clear personnel within the immediate area, making sure to follow the appropriate standoff distance guidelines displayed in Table 2.

9. Tare the load cell, set desired sampling rate to “1200 sps”, and begin recording load cell force measurements.
10. Countdown from 5 and start ignition sequence in LabVIEW.
11. Once test has been completed, disconnect wire leads from power source and end data collection. Allow motor to be cool to the touch before removing motor from thrust stand by releasing clamps and begin disposal of single-use parts.

Table 2: National Associsation of Rocketry (NAR) Standoff Distances for High Powered Motor Testing [37]

Installed Total Impulse (Newton-Seconds)	Equivalent High Power Motor Type	Minimum Diameter of Cleared Area (ft.)	Minimum Personnel Distance (ft.)	Minimum Personnel Distance (Complex Rocket) (ft.)
0 — 320.00	H or smaller	50	100	200
320.01 — 640.00	I	50	100	200
640.01 — 1,280.00	J	50	100	200
1,280.01 — 2,560.00	K	75	200	300
2,560.01 — 5,120.00	L	100	300	500
5,120.01 — 10,240.00	M	125	500	1000
10,240.01 — 20,480.00	N	125	1000	1500
20,480.01 — 40,960.00	O	125	1500	2000

Note: A Complex rocket is one that is multi-staged or that is propelled by two or more rocket motors

3.4 Propellant Formulation

The baseline of the propellant formulation used within this study is outlined in this section. Slight variances in ammonium perchlorate and aluminum ratios are tested throughout the study, but all formulations are referenced off of the one mentioned here. Content percent weight ratios remain constant throughout for the ingredients of; copper chromite, HTPB, tepanol, DOA, castor oil, and the IDPI curative. For the specific ratios of ammonium perchlorate particle sizes within each test or variances in ammonium perchlorate and aluminum content, refer to Appendix A.2 and Table 4 to observe the preliminary and final test matrices. The baseline propellant formulation referenced against total percent weight of the mixture is as follows:

- Ammonium Perchlorate (90 µm, 200 µm, 400 µm): 75.80%
- Aluminum 325 mesh (44 µm): 5.02%
- HTPB (R45 HTLO) and Minor Additives: 19.18%

CHAPTER IV

RESULTS

4.1 Propellant Manufacturing Results

Table 5 and Table 6 display each recorded motor physical property throughout all tests where ammonium perchlorate average particle sizes and ratios were altered. Assessing the quality of a manufactured motor is important to note before testing can begin. As mentioned before, comparison between theoretical and manufactured propellant density is the least invasive way to assess propellant quality. It is from observed physical characteristics that an average particle size corresponding to an average ammonium perchlorate size of 261 μm was chosen to be applied to variances in aluminum total content. Additionally, a 2 grain motor configuration was chosen as a result of observed performance qualities that will be further expanded upon later. Thus, the full final version of the preliminary test matrix displayed in Appendix A.2 can be viewed in Table 4. Theoretical values for propellant densities were attained through a software known as ProPEP 3. ProPEP allows for propellant compositions to be defined in order to estimate resulting physical and chemical properties as displayed in Figure 19 below. Theoretical physical properties for each case can be observed in Table 3.

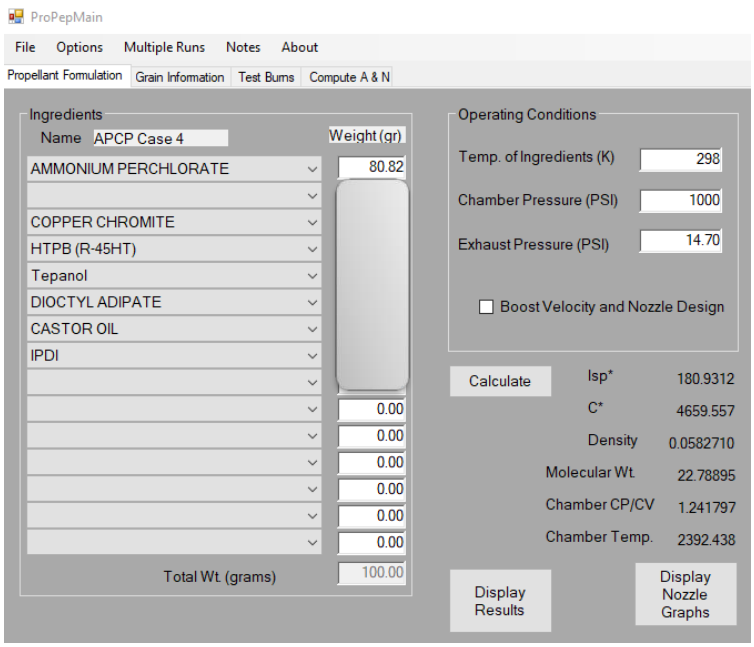

Figure 19: ProPEP 3 Interface for Acquiring Theoretical Propellant Physical and Chemical Properties

Table 3: ProPEP 3 Theoretical Propellant Densities for Tested Formulations

Total AP/AL Included (%)	Theoretical Density (lbm/in^3)
80.82/0.00	0.0583
75.80/5.02	0.0599
70.78/10.04	0.0606

Table 4: Final APCP Motor Test Matrix

	Composition Variable	Test #	AP % 90	AP % 200	AP % 400	AP % Tot	AL % Tot	Total Grain #	L per Grain (in)	Prop Total L (in)
	AP Equal	1.1a	25.27	25.27	25.27	75.80	5.02	3	2.225	6.675
		1.2a	25.27	25.27	25.27	75.80	5.02	3	2.225	6.675
		1.3a	25.27	25.27	25.27	75.80	5.02	3	2.225	6.675
		1.4b	25.27	25.27	25.27	75.80	5.02	2	3.3375	6.675
		1.5b	25.27	25.27	25.27	75.80	5.02	2	3.3375	6.675
Config. 1 Total:	6	1.6b	25.27	25.27	25.27	75.80	5.02	2	3.3375	6.675
	AP90 - 10%	2.1a	15.27	25.27	35.27	75.80	5.02	3	2.225	6.675
		2.2a	15.27	25.27	35.27	75.80	5.02	3	2.225	6.675
		2.3a	15.27	25.27	35.27	75.80	5.02	3	2.225	6.675
		2.4b	15.27	25.27	35.27	75.80	5.02	2	3.3375	6.675
		2.5b	15.27	25.27	35.27	75.80	5.02	2	3.3375	6.675
Config. 2 Total:	6	2.6b	15.27	25.27	35.27	75.80	5.02	2	3.3375	6.675
	AP90 + 10%	3.1a	35.27	25.27	15.27	75.80	5.02	3	2.225	6.675
		3.2a	35.27	25.27	15.27	75.80	5.02	3	2.225	6.675
		3.3a	35.27	25.27	15.27	75.80	5.02	3	2.225	6.675
		3.4b	35.27	25.27	15.27	75.80	5.02	2	3.3375	6.675
		3.5b	35.27	25.27	15.27	75.80	5.02	2	3.3375	6.675
Config. 3 Total:	6	3.6b	35.27	25.27	15.27	75.80	5.02	2	3.3375	6.675
	AP90 -10% (261 µm) with 2 Total Grains									
	Composition Variable	Test #	AP % 90	AP % 200	AP % 400	AP % Tot	AL % Tot	Total Grain #	L per Grain (in)	Prop Total L (in)
	AL - 5%	4.1	16.28	26.94	37.61	80.82	0	2	3.3375	6.675
		4.2	16.28	26.94	37.61	80.82	0	2	3.3375	6.675
Config. 4 Total:	3	4.3	16.28	26.94	37.61	80.82	0	2	3.3375	6.675
	AL + 5.0%	5.1	14.26	23.59	32.93	70.78	10.04	2	3.3375	6.675
		5.2	14.26	23.59	32.93	70.78	10.04	2	3.3375	6.675
Config. 5 Total:	3	5.3	14.26	23.59	32.93	70.78	10.04	2	3.3375	6.675
Grand Total:	24									

Table 5: Ammonium Perchlorate Particle Size Variation Physical Properties

Test	Total Grains	Average AP Particel Size (um)	Propellant Mass (grams)	Average Density (lbm/in^3)	Average Density Error (%)
1.1a	3	230	386.06	0.0573	4.43%
1.2a	3	230	400.04	0.0587	2.02%
1.3a	3	230	400.40	0.0585	2.24%
1.4b	2	230	402.41	0.0587	1.92%
1.5b	2	230	394.47	0.0580	3.17%
1.6b	2	230	391.73	0.0573	4.39%
2.1a	3	261	408.12	0.0598	0.25%
2.2a	3	261	401.60	0.0589	1.52%
2.3a	3	261	404.11	0.0594	0.72%
2.4b	2	261	404.12	0.0591	1.29%
2.5b	2	261	402.64	0.0587	1.91%
2.6b	2	261	407.66	0.0595	0.52%
3.1a	3	199	392.19	0.0573	4.33%
3.2a	3	199	392.32	0.0574	4.21%
3.3a	3	199	391.16	0.0571	4.69%
3.4b	2	199	391.10	0.0570	4.83%
3.5b	2	199	394.23	0.0575	4.21%
3.6b	2	199	398.85	0.0581	4.69%

Table 6: Aluminum Variation Physical Properties at 261 µm Ammonium Perchlorate Average Particle Size

Test	Total Grains	Total AP/AL Included (%)	Propellant Mass (grams)	Average Density (lbm/in^3)	Average Density Error (%)
4.1	2	80.82/0.00	391.92	0.0572	1.90%
4.2	2	80.82/0.00	389.84	0.0572	1.78%
4.3	2	80.82/0.00	392.22	0.0573	1.70%
2.4b	2	75.80/5.02	404.12	0.0591	1.29%
2.5b	2	75.80/5.02	402.64	0.0587	1.91%
2.6b	2	75.80/5.02	407.66	0.0595	0.52%
5.1	2	70.78/10.04	408.61	0.0596	1.58%
5.2	2	70.78/10.04	406.64	0.0594	2.06%
5.3	2	70.78/10.04	406.65	0.0594	2.00%

Table 7 and Table 8 below show results of motor density comparison and consistency through each individual variation in average ammonium perchlorate particle size and content ratio. A 261 µm ammonium perchlorate average particle size, on average, most closely agreed with its theoretical density value at a 75.80% ammonium perchlorate content. This is observed in that case 2 motors had an average error of 1.03%. However, when aluminum content was varied, the deviation of density values reduced to 0.26% at a 10.04% aluminum content and minimized to a 0.10% deviation with no aluminum present in the formulation. Thus, density consistency improved both when aluminum content was increased and decreased. Motors with a 199 µm particle size on average deviated most heavily with its theoretical value, while 230 µm motors were the most variable with each other. Figures for observing general density trends over average

ammonium perchlorate particle sizes and content ratios can be observed in Appendix A.3 and A.4.

Table 7: Physical Properties at Varying Ammonium perchlorate Particle Sizes

Test	Average AP Particel Size (um)	Average Density (lbm/in^3)	Density (% Stdv)	Average Desnity Error (% Error)
1	230	0.0581	1.16%	3.03%
2	261	0.0593	0.67%	1.03%
3	199	0.0574	0.69%	4.50%

Table 8: Physical Properties at Varying Ratios of Ammonium Perchlorate and Aluminum

Test	Total AP/AL Included (%)	Average Density (lbm/in^3)	Density (% Stdv)	Average Desnity Error (% Error)
4	80.82/0.00	0.0572	0.10%	1.79%
5	70.78/10.04	0.0595	0.26%	1.88%

4.2 Test Results Overview

4.2.1 Case 1: 230 µm Results

Figure 20and Figure 21 show thrust curve profiles against burn time for motors with average ammonium perchlorate particle sizes of 230 µm in both 2 and 3 grain configurations. For 230 µm 3 grain motors, a relatively neutral initial thrust profile is observed throughout the first half of each motor's burn. After this, a regressive burn behavior is observed for the remaining duration of each thrust profile. All motors have burn times within 2.5 seconds with peak thrust reaching maximum values near the 1.0 second mark. Also, initial peak thrust values seem to vary between 90 lbf and 115 lbf.

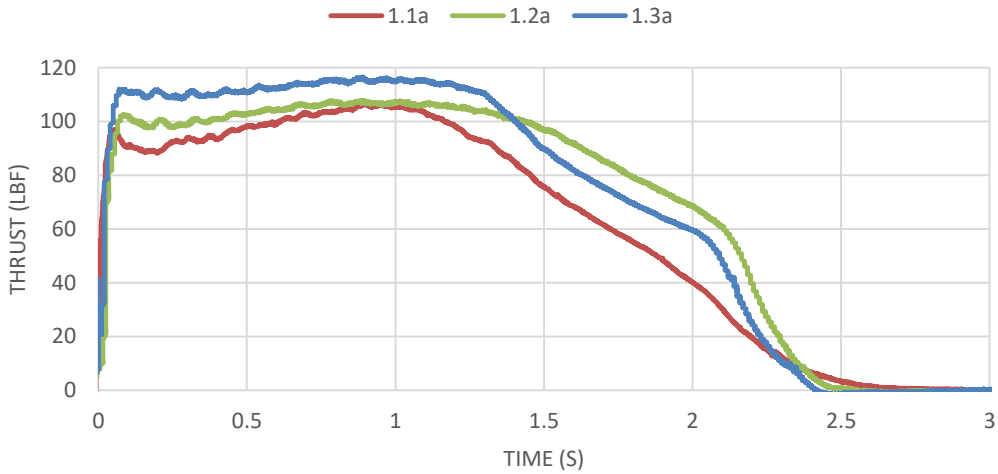

Figure 20: 230 µm Ammonium Perchlorate Average Size Motor Performance for 3 Grain Configuration

Motors with a 230 µm ammonium perchlorate size in a 2 grain configuration exhibited progressive burn profiles in all cases. As observed for motors of this particle size with a 3 grain configuration, all motors have burn times that appear to be very close 2.5 seconds. However, while peak thrust values of 3 grain motors occurred near the 1.0 second mark, 2 grain configured motors did not peak until around 2.0 seconds after ignition, much closer to the end of the motor's burn time. Initial thrust rise appears to be quite consistent, ranging between 70 lbf and 80 lbf.

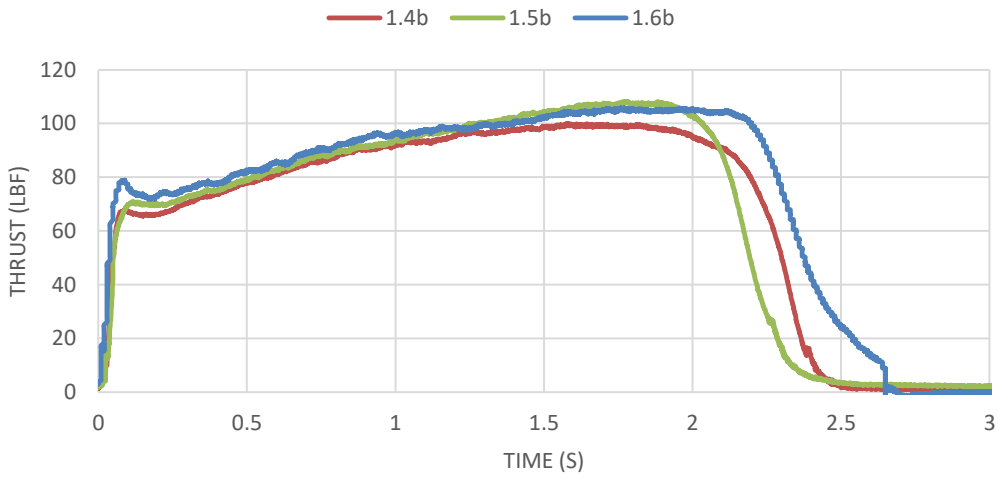

Figure 21: 230 µm Ammonium Perchlorate Average Size Motor Performance for 2 grain Configuration

4.2.2 Case 2: 261 µm Results

Figure 22 and Figure 23 show thrust curve profiles against burn time for motors with ammonium perchlorate average particle sizes of 261 µm in both 2 and 3 grain configurations. For 261 µm 3 grain motors, a slightly regressive burn behavior is observed for each thrust profile. All motors exhibited burn times slightly above or below 3.0 seconds with peak thrust reaching maximum values during the initial rise portion of their thrust curves in two out of the three tests. Initial rise of each motor spans between 70 lbf and 115 lbf.

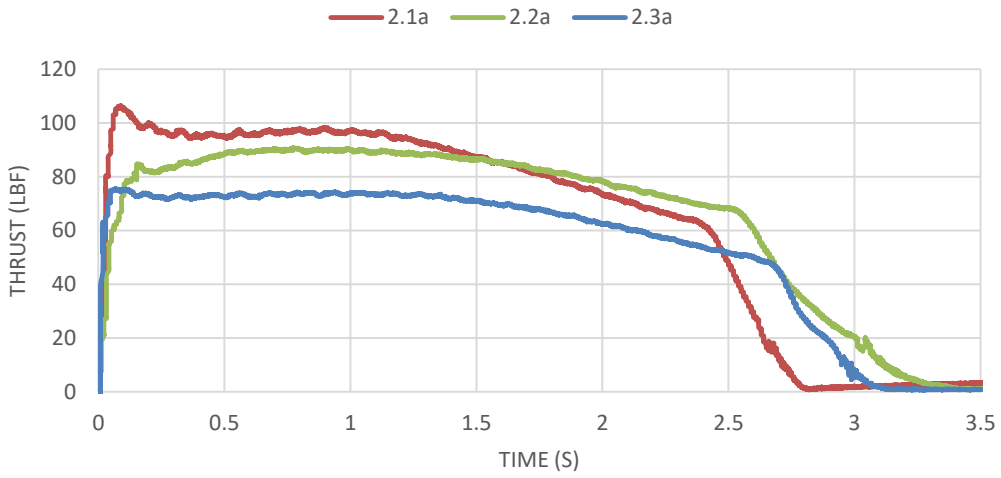

Figure 22: 261 µm Ammonium Perchlorate Average Size Motor Performance for 3 grain Configuration

For cases of 261 µm ammonium perchlorate sizes in a 2 grain configuration, progressive burn profiles in all cases were observed just as in what was displayed for the 230 µm 2 grain configurations. Similar to motors of 261 µm average particle size with a 3 grain configuration, all 2 grain configured motors have burn times that appear to be very close 3.0 seconds. Peak thrust values of 261 µm 2 grain configured motors did not peak until closer to the end of their burn time, all occurring at about the 2.0 second mark. Case 2.6b was the exception to this, as it peaked right at the very end of its burn. Initial thrust rise is relatively consistent and within the range of 60 lbf to 70 lbf.

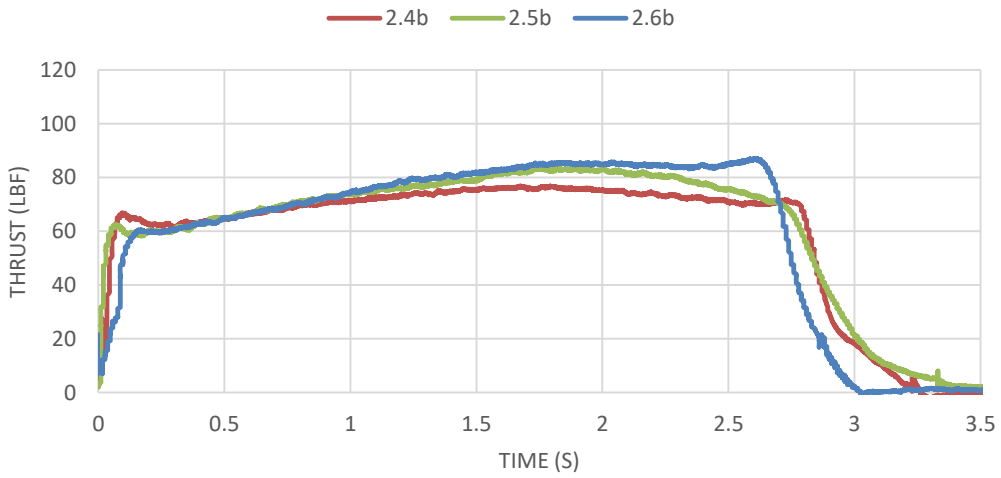

Figure 23: 261 µm Ammonium Perchlorate Average Size Motor Performance for 2 grain Configuration

4.2.3 Case 3: 199 µm Results

Figure 24 and Figure 25 show burn profiles for motors with average ammonium perchlorate particle sizes of 199 µm in both 2 and 3 grain configurations. For 199 µm 3 grain motors, a burn behavior similar to what was observed for 3 grain 230 µm motors is observed. An initial neutral or slightly progressive profile is present, followed by a heavy regressive behavior. All motors exhibited burn times slightly above or between 2.0 and 2.5 seconds with peak thrust reaching maximum values at around the 1.0 second point in all three tests. The initial peak for motors observed below appears to range between 100 lbf and 120 lbf.

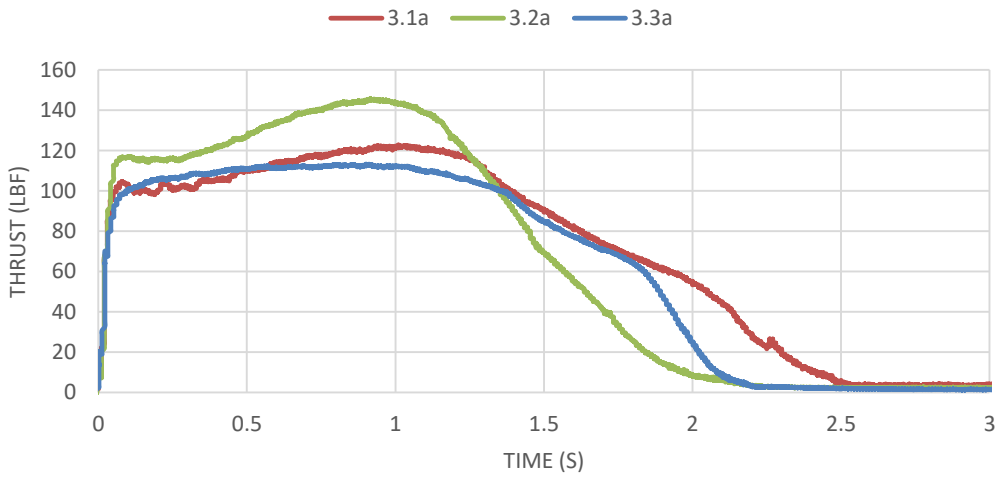

Figure 24: 199 µm Ammonium Perchlorate Average Size Motor Performance for 3 grain Configuration

For 199 µm ammonium perchlorate average sizes in a 2 grain configuration, progressive burn profiles in all cases were observed just as in what was displayed for 261 µm and 230 µm 2 grain configurations. Similar to motors of a 199 µm particle size with a 3 grain configuration, all 2 grain configured motors have burn times that appear to land between 2.0 and 2.5 seconds. Peak thrust values of 199 µm 2 grain configured motors peaked closer to the end of their burn times, with case 3.6b peaking at the very end of its burn. Initial peak thrust appears to be fairly consistent with each motor producing around 75 lbf.

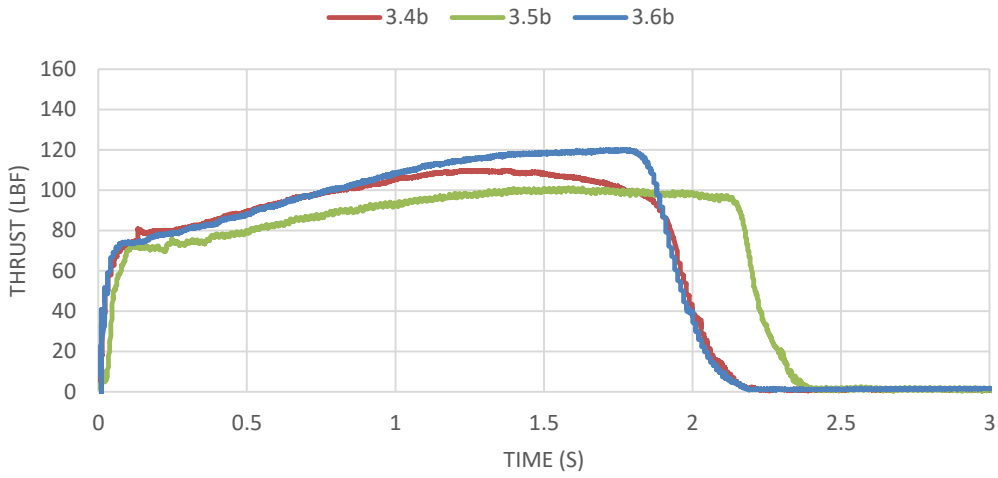

Figure 25: 199 µm Ammonium Perchlorate Average Size Motor Performance for 2 grain Configuration

4.2.4 Case 4: 261 µm, 0% AL Results

As mentioned before, a 261 µm ammonium perchlorate average particle size was selected and carried over to tests where aluminum content was varied. This partly was due to favorable physical characteristics as it resulted in the highest observed average motor densities, but also partly due to the stark contrast between the thrust profiles of the two and three grain configurations. 3 grain configurations all exhibited similar overall behaviors, but initial thrust peaks looked very dissimilar and the courses of each thrust profile didn't follow similar paths with regards to thrust and time values. However, all the inconsistencies observed between the 3 grain configurations are largely not present for the 2 grain configurations. Cases for motors within the 2b category had similar initial thrust peaks, and had similar thrust slopes. However, some differences arise near the last third of each motor's burn profile with regards to peak thrust. Thus, a 2 grain configuration and a 261 µm ammonium perchlorate size was chosen for further evaluation for performance variances when aluminum content is varied.

Figure 26 displays the burn profiles for motors with average ammonium perchlorate particle sizes of 261 µm in a 2 grain configuration, while containing no aluminum within the formulation. The burn behaviors of these motors appears strangely erratic. Motors 4.1 and 4.3 show fairly progressive thrust profiles while 4.2 portrays an initial progressive and then later

heavy regressive burn behavior. There also doesn't appears to be much uniformity between motor burn times or maximum thrust locations.

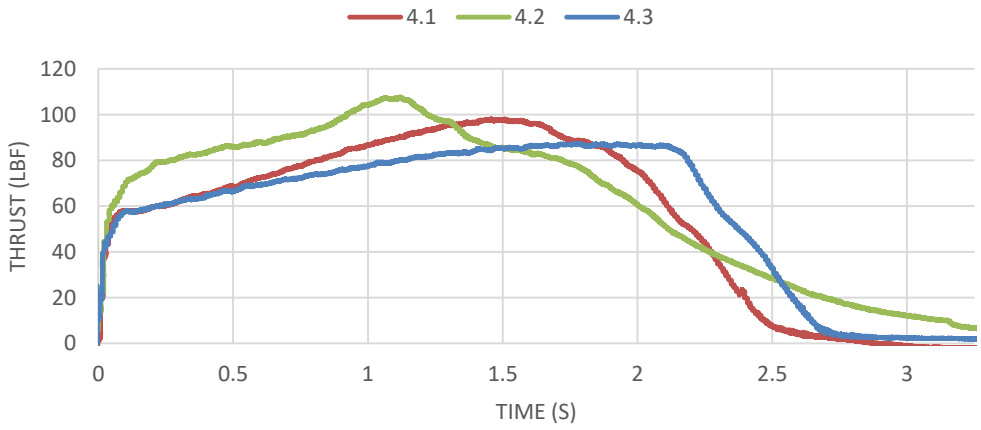

Figure 26: 261 µm Ammonium Perchlorate Average Size Motor Performance for 2 grain Configuration at a 0% Aluminum Content

4.2.5 Case 5: 261 µm, 10% AL Results

Figure 27 displays the burn profiles for motors with ammonium perchlorate average particle sizes of 261 µm in a 2 grain, while containing a 10% aluminum content. The erratic burn behaviors observed for the case where no aluminum was present have almost been completely eliminated. In fact, it appears off of first glance that the motors within this formulation have the most similarities with each other than what has been observed in other cases. All motors have burn times sitting around the 3.50 second mark and display a neutral-progressive burn profile shape. Additionally, all peak thrust values occur around the 2.0 second mark and are nearly equal in magnitude. Initial rise in thrust shows to be very consistent and is within 55 lbf to 60 lbf range in all cases.

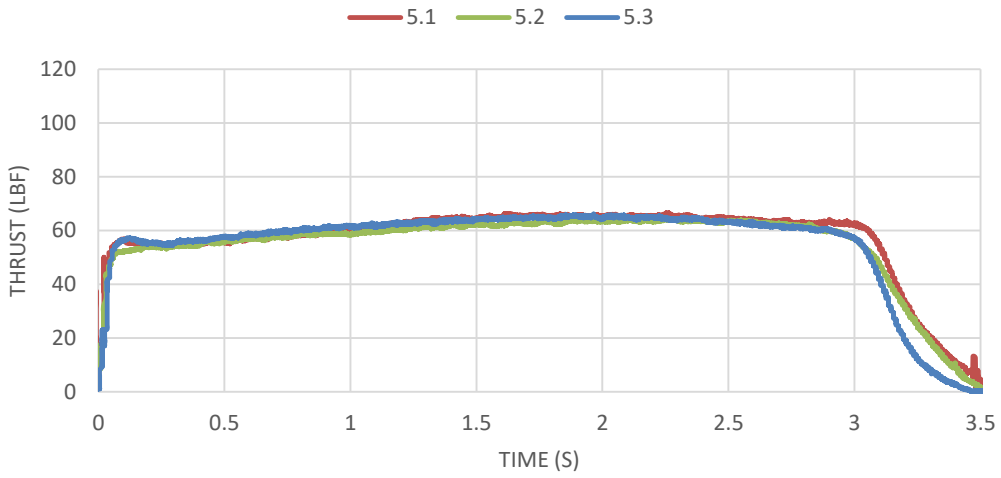

Figure 27: 261 µm Ammonium Perchlorate Average Size Motor Performance for 2 grain Configuration at a 10% Aluminum Content

4.3 Performance Parameter Results and Analysis

Table 9 displays all performance parameter results over the various ammonium perchlorate average particle sizes and aluminum content percentages. The charts immediately provide serve as an overview of all tests and how they performed on measures related to key performance parameters alone. While identifying trends in performance parameters is not the focus of this study, it is important to realize that different grain lengths and granular distributions, related to ammonium perchlorate particle size and total aluminum content, will result in different performance behaviors. It is also important to note that this study is intended to enhance the predictability of future APCP's by identifying granular and geometric motor tendencies related to performance consistency. Thus, general performance trends regarding each configured set of motors will be observed, and curve fits of average motor performance will be identified in order to capture general performance behaviors that can be applied in future works. Polynomial curve fits in particular were chosen because a change in average ammonium perchlorate size is effectively a change in the average burning surface area of the ammonium perchlorate particles. The same reasoning applies for changes in total ammonium perchlorate and aluminum ratios, the

effective particle burning surface area is changing with an increase or decreased in aluminum or ammonium perchlorate content.

Table 9: Performance Parameters for Variations in Ammonium Perchlorate Particle Size (Top) and Aluminum Content (Bottom)

Test	Average AP Particel Size (um)	Propellant Mass (grams)	Peak Thrust (lbf)	Average Thrust (lbf)	Burn Time (s)	Total Impulse (lbf*s)	Specific Impulse (s)
1.1a	230	386.06	106.70	78.00	2.31	180.10	211.60
1.2a	230	400.04	107.84	89.82	2.31	207.48	235.26
1.3a	230	400.40	116.52	92.90	2.26	209.96	237.85
1.4b	230	402.41	100.04	84.13	2.37	199.30	224.64
1.5b	230	394.47	108.22	87.24	2.28	198.65	228.42
1.6b	230	391.73	105.91	85.69	2.60	222.79	257.98
2.1a	261	408.12	106.48	81.85	2.69	220.25	244.80
2.2a	261	401.60	90.87	73.67	3.07	226.23	255.52
2.3a	261	404.11	75.64	62.78	2.99	187.72	210.71
2.4b	261	404.12	76.84	66.06	3.10	204.44	229.47
2.5b	261	402.64	83.70	67.98	3.15	214.22	241.33
2.6b	261	407.66	87.14	73.06	2.85	207.85	231.27
3.1a	199	392.19	122.79	89.62	2.34	209.72	242.55
3.2a	199	392.32	145.73	106.27	1.87	198.73	229.77
3.3a	199	391.16	113.26	92.82	2.04	189.35	219.57
3.4b	199	391.10	109.96	92.01	2.08	191.01	221.54
3.5b	199	394.23	101.29	86.66	2.26	196.21	225.75
3.6b	199	398.85	120.33	96.47	2.05	197.76	224.90

Test	Total AP/AL Included (%)	Propellant Mass (grams)	Peak Thrust (lbf)	Average Thrust (lbf)	Burn Time (s)	Total Impulse (lbf*s)	Specific Impulse (s)
4.1	80.82/0.00	391.92	98.22	73.38	2.45	179.78	208.06
4.2	80.82/0.00	389.84	107.70	66.02	3.06	201.97	234.99
4.3	80.82/0.00	392.22	87.36	70.44	2.62	184.56	213.43
5.1	70.78/10.04	408.61	66.65	57.47	3.45	198.16	219.98
5.2	70.78/10.04	406.64	64.59	56.42	3.39	191.25	213.33
5.3	70.78/10.04	406.65	66.18	58.28	3.28	191.15	213.22

Hypothesis testing through a series of F-tests was conducted at a 90% confidence level for all discussed performance parameters, with p-values being tabulated for one-sided testing of equal variances. P-values less than 0.1 indicate that a difference in sample variance is present to a 90% confidence level and are highlighted in green. P-values less than 0.2 have been highlighted yellow in order to indicate that the potential for differences in sample variance exists and more testing should be conducted. Testing for equal sample variance was conducted for cases of 3 grain geometries with varying ammonium perchlorate average particle sizes, 2 grain geometries with varying ammonium perchlorate average particle sizes, 3 versus 2 grain geometries at equal ammonium perchlorate average particle sizes, and for varying aluminum content percentages at a constant average ammonium perchlorate particle size equal to 261 μm.

4.3.1 Peak Thrust

Average values of peak thrust achieved for each motor configuration can be observed in Table 10 along with their respective percent standard deviations.

Table 10: Peak Thrust Performance for Variations in Ammonium Perchlorate Particle Size (Top) and Aluminum Content (Bottom)

Test	Average AP Particel Size (um)	Average Peak Thrust (lbf)	Peak Thrust (% Stdv)
1a	230	110.35	4.86%
1b	230	104.72	4.03%
2a	261	91.00	16.94%
2b	261	82.56	6.36%
3a	199	127.26	13.12%
3b	199	110.53	8.62%

Test	Total AP/AL Included (%)	Average Peak Thrust (lbf)	Peak Thrust (% Stdv)
4	80.82/0.00	97.76	10.41%
5	70.78/10.04	65.81	1.64%

Upon observation of average peak thrust values verses average ammonium perchlorate size, it appears that there is an inverse proportionality between the two as what can be observed by Figure 28. Higher average particle sizes resulted in a general decrease in observed peak thrust values overall. This trend is noticeable for both 3 grain and 2 grain motor configurations. Through the use of linear regression model analysis, 3 grain tests demonstrated that 64.34% of peak thrust values were linearly correlated to average particle size while 2 grain tests produced a value of 74.29% when the individual peak thrust values of each test were taken into consideration. This indicates a moderate-strong linear correlation between peak thrust and average ammonium perchlorate particle size.

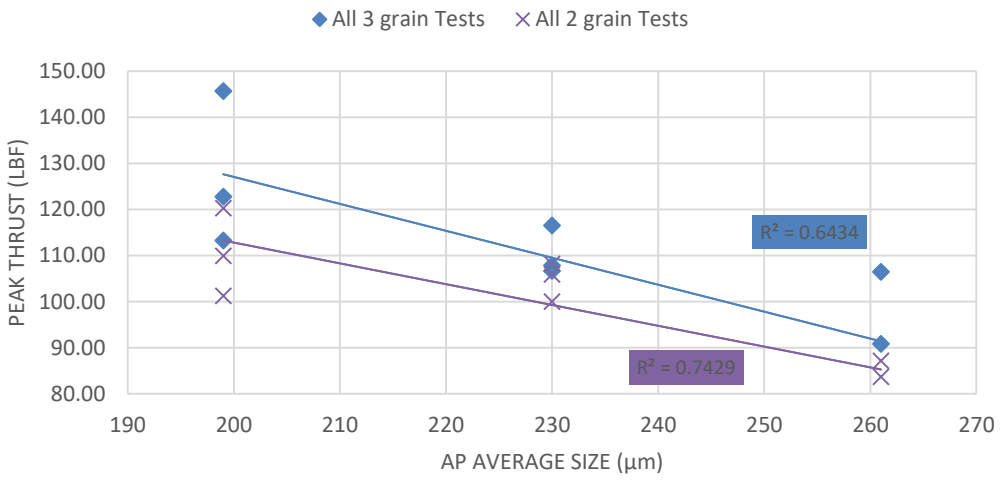

Figure 28: Peak Thrust vs. AP Average Size for All Tests

Figure 29 displays second order polynomial curve fits for the averages of peak thrust against ammonium perchlorate particle size for 3 grain and 2 grain configurations that can be used in future modeling of performance predictability.

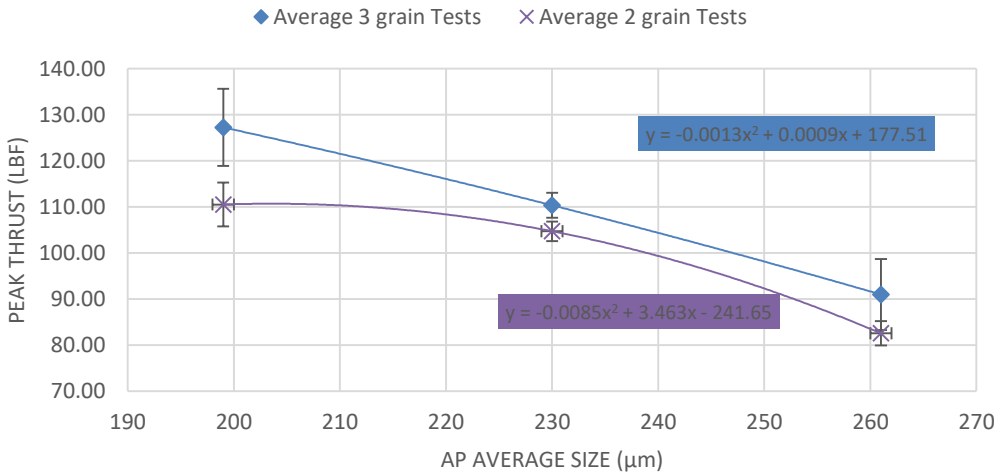

Figure 29: Average Peak Thrust vs. AP Average Size

Figure 30 shows that a similar trend is observed for peak thrust values as a function of ammonium perchlorate and aluminum content percentages. An increased in peak thrust was observed with an increase in ammonium perchlorate content percentage, meaning a decrease in aluminum percentage, with an 85.22% linear correlation when all peak thrust values were plotted for each test.

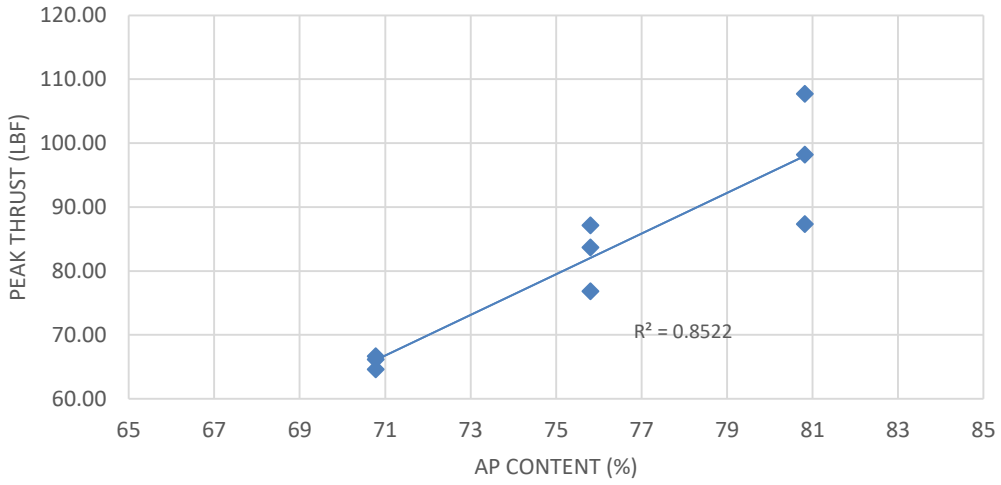

Figure 30: Peak Thrust vs. AP/AL Content Variation for All Tests

Figure 31 displays a second order polynomial curve fit for the averages of peak thrust against ammonium perchlorate content percentage that can be used in future modeling of performance predictability.

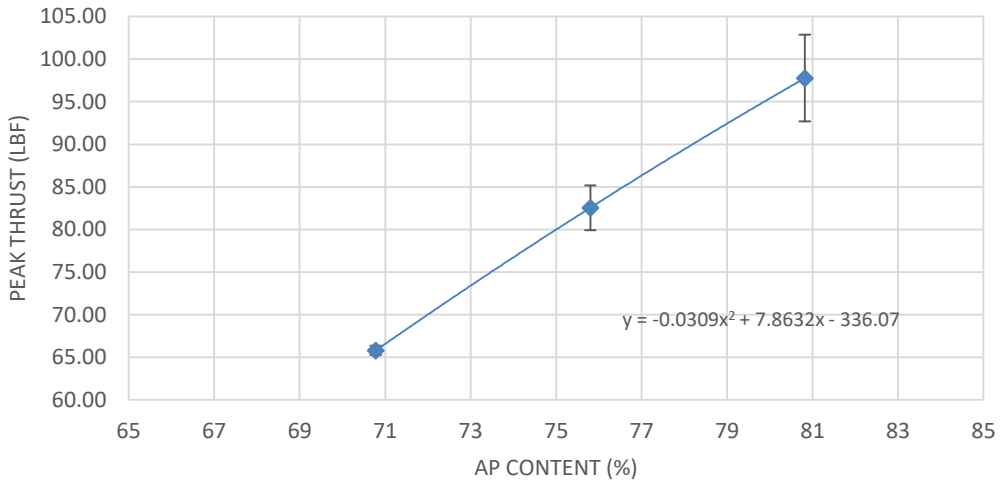

Figure 31: Average Peak Thrust vs. AP/AL Content Variation

Table 11 through Table 14 below shows results from null-hypothesis testing of motor configuration peak thrust variances. In comparison of 3 grain geometries at the varying sizes of ammonium perchlorate particles, the variance in peak thrust at 230 µm proved to be significantly less than that observed for 199 µm while also providing the potential to be less than the variance

observed for 261 µm motors. No significant differences in peak thrust variances were observed between 2 grain geometries of varying ammonium perchlorate particle sizes, but evidence suggests that there could be a peak thrust variance reduction in 230 µm motors compared to 199 µm. Comparison of 3 versus 2 grain configurations at constant average ammonium perchlorate particle sizes gave no significant differences in peak thrust, but there is cause for the possibility that a variance reduction in 2 grain compared to 3 grain motors exists for an ammonium perchlorate particle size of 261 µm. Equal peak thrust variance testing for cases where aluminum and ammonium perchlorate content ratios were altered showed a significant reduction in peak thrust variance at an aluminum weight fraction of 10.04% compared to aluminum content formulations of 5.02% and 0%.

Table 11: Peak Thrust Equal Variance Results for 3 Grain Configured Motors at Equal AP Average Size

Comparison: 3 grain Geometries	P Value (one Tail)	Variance Variable 1	Variance Variable 2
1a (230 µm) - 2a (261 µm)	0.11	28.81	237.74
1a (230 µm) - 3a (199 µm)	0.09	28.81	278.59
2a (261 µm) - 3a (199 µm)	0.46	237.74	278.59

Table 12: Peak Thrust Equal Variance Results for 2 Grain Configured Motors at Equal AP Average Size

Comparison: 2 grain Geometries	P Value (one Tail)	Variance Variable 1	Variance Variable 2
1b (230 µm) - 2b (261 µm)	0.39	17.79	27.53
1b (230 µm) - 3b (199 µm)	0.16	17.79	90.79
2b (261 µm) - 3b (199 µm)	0.23	27.53	90.79

Table 13: Peak Thrust Equal Variance Results for 3 vs. 2 Grain Configured Motors at Equal AP Average Size

Comparison: 3 grain vs. 2 grain	P Value (one Tail)	Variance Variable 1	Variance Variable 2
1a (230 µm) - 1b (230 µm)	0.38	28.81	17.79
2a (261 µm) - 2b (261 µm)	0.10	237.74	27.53
3a (199 µm) - 3b (199 µm)	0.25	278.59	90.79

Table 14: Peak Thrust Equal Variance Results at a 261 µm AP Average Size for Varying AP/AL Content Ratios

Comparison: 261 µm Tests	P Value (one Tail)	Variance Variable 1	Variance Variable 2
2b (5.02% AL) - 4 (0% AL)	0.21	27.53	103.54
2b (5.02% AL) - 5 (10.04% AL)	0.04	27.53	1.17
4 (0% AL) - 5 (10.04% AL)	0.01	103.54	1.17

4.3.2 Average Thrust

Calculated values of average thrust achieved for each motor configuration can be observed in Table 15 along with their respective percent standard deviations.

Table 15: Average Thrust Performance for Variations in Ammonium Perchlorate Particle Size (Top) and Aluminum Content (Bottom)

Test	Average AP Particel Size (um)	Average Thrust (lbf)	Average Thrust (% Stdv)
1a	230	86.91	9.05%
1b	230	85.69	1.82%
2a	261	72.77	13.14%
2b	261	69.03	5.24%
3a	199	96.24	9.18%
3b	199	91.71	5.35%

Test	Total AP/AL Included (%)	Average Thrust (lbf)	Average Thrust (% Stdv)
4	80.82/0.00	69.95	5.29%
5	70.78/10.04	57.39	1.63%

Observation of average thrust values verses average ammonium perchlorate size appears to indicate that the two are inversely proportional by what is observed in Figure 32. Higher particle sizes resulted in a general decrease in observed average thrust values, which is the same general trend observed for peak thrust values. This trend is noticeable for both 3 grain and 2 grain motor configurations. A 63.53% direct correlation between average thrust and average ammonium perchlorate particle size was observed for 3 grain tests, while 2 grain tests produced a value of 85.05%. This indicates a moderate-strong linear correlation between average motor thrust and ammonium perchlorate particle size.

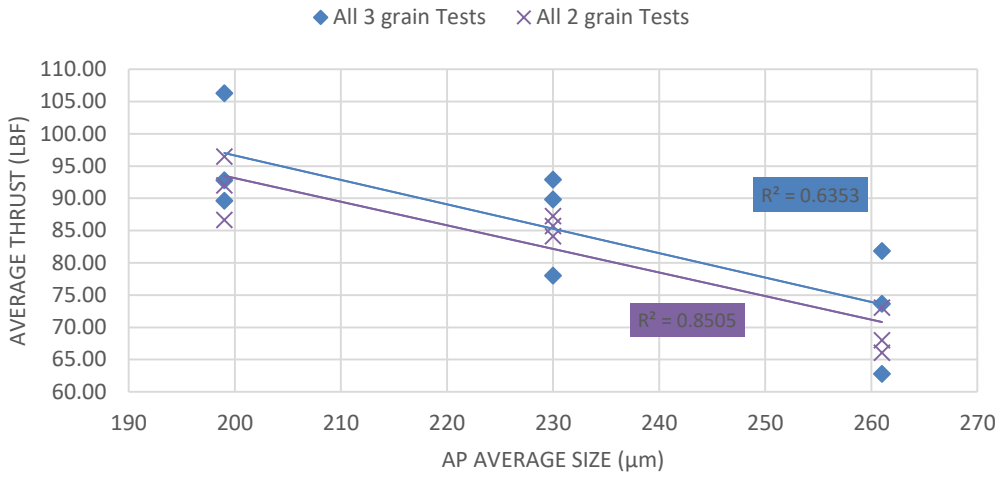

Figure 32: Average Thrust vs. AP Average Size for All Tests

The second order polynomial curve fits in Figure 33 show averages of motor average thrust against ammonium perchlorate particle average size for 3 grain and 2 grain configurations that can be used in future modeling of performance predictability.

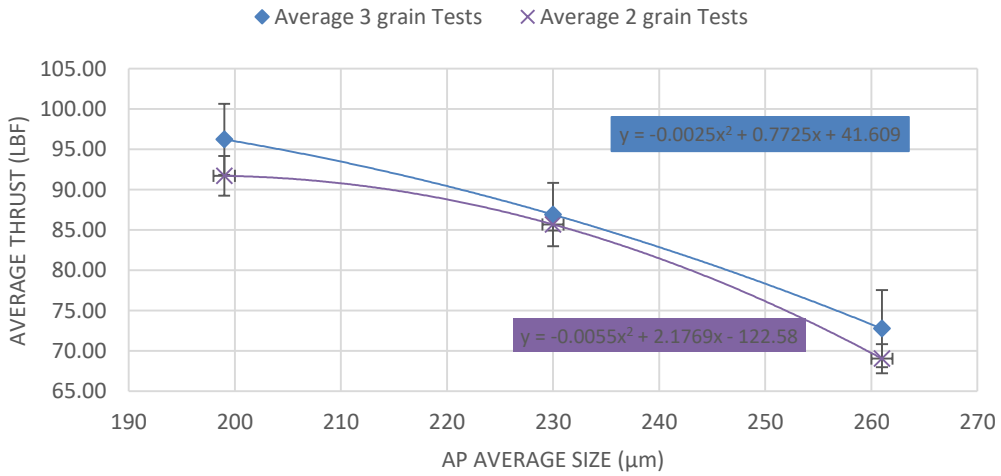

Figure 33: Average Configured Motor Thrust vs. AP Average Size

Figure 34 shows that a similar trend is observed for average thrust values as a function of ammonium perchlorate and aluminum content percentages. A moderate Increase in average thrust was observed with an increase in ammonium perchlorate content percentage. This is observed with a 67.70% linear correlation when all average thrust values were plotted for each test.

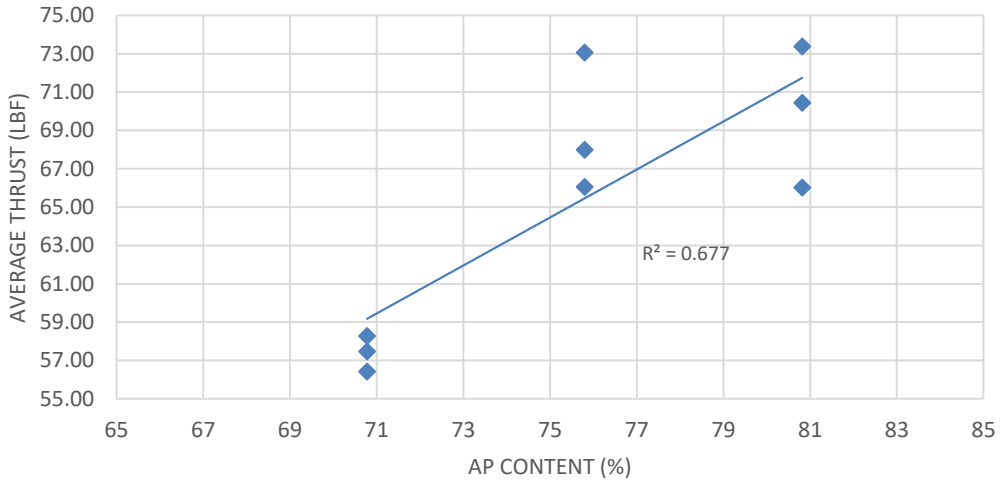

Figure 34: Average Thrust vs. AP/AL Content Variation for All Tests

Figure 35 displays the second order polynomial curve fit for motor configuration average thrust against ammonium perchlorate content percentage that can be used in future modeling of average thrust predictability.

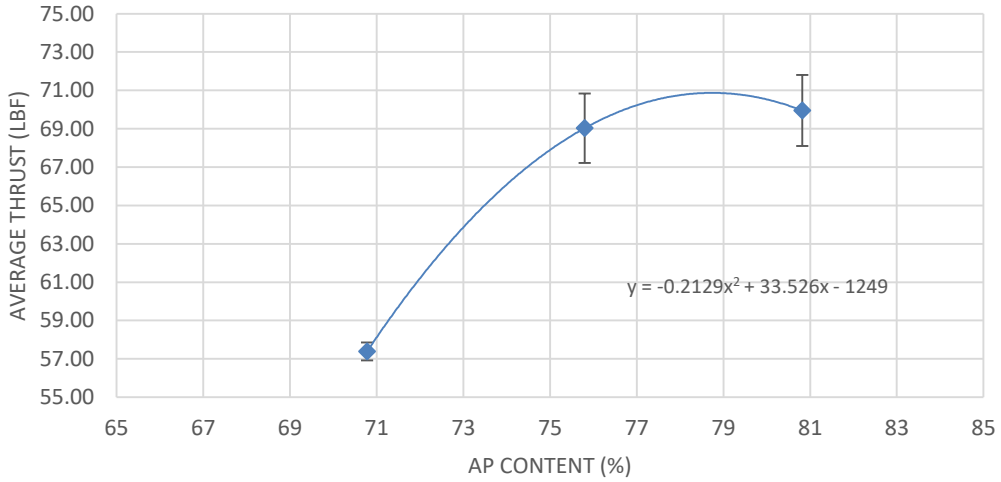

Figure 35: Average Configured Motor Thrust vs. AP/AL Content Variation

Table 16 through Table 19 show results of equal variance hypothesis testing for configured motor average thrust values. In comparison of 3 grain geometries at the varying sizes of ammonium perchlorate particle sizes, there were no significant or potentially promising differences in variances of motor average thrust at differing particle sizes of ammonium perchlorate. Significant differences in average thrust variances were observed between 2 grain

geometries, where 230 µm tests varied less than 199 µm tests. Also, evidence suggests that there could be an average thrust variance reduction in 230 µm motors compared to 261 µm. Comparison of 3 versus 2 grain configurations at constant ammonium perchlorate particle sizes gave significant differences in variance of average thrust, where 2 grain 230 µm motors varied less than 3 grain. There is cause for the possibility that an average thrust variance reduction in 2 grain compared to 3 grain motors exists for an average ammonium perchlorate particle size of 261 µm. Variance testing for cases where aluminum and ammonium perchlorate content ratios were changed showed a significant reduction in average thrust variance at an aluminum weight fraction of 10.04% compared to aluminum content formulations of 5.02% and 0%.

Table 16: Average Thrust Equal Variance Results for 3 Grain Configured Motors at Equal AP Average Size

Comparison: 3 grain Geometries	P Value (one Tail)	Variance Variable 1	Variance Variable 2
1a (230 µm) - 2a (261 µm)	0.40	61.89	91.47
1a (230 µm) - 3a (199 µm)	0.44	61.89	78.09
2a (261 µm) - 3a (199 µm)	0.46	91.47	78.09

Table 17: Average Thrust Equal Variance Results for 2 Grain Configured Motors at Equal AP Average Size

Comparison: 2 grain Geometries	P Value (one Tail)	Variance Variable 1	Variance Variable 2
1b (230 µm) - 2b (261 µm)	0.16	2.43	13.09
1b (230 µm) - 3b (199 µm)	0.09	2.43	24.10
2b (261 µm) - 3b (199 µm)	0.35	13.09	24.10

Table 18: Average Thrust Equal Variance Results for 3 vs. 2 Grain Configured Motors at Equal AP Average Size

Comparison: 3 grain vs. 2 grain	P Value (one Tail)	Variance Variable 1	Variance Variable 2
1a (230 µm) - 1b (230 µm)	0.04	61.89	2.43
2a (261 µm) - 2b (261 µm)	0.13	91.47	13.09
3a (199 µm) - 3b (199 µm)	0.24	78.09	24.10

Table 19: Average Thrust Equal Variance Results at a 261 µm AP Average Size for Varying AP/AL Content Ratios

Comparison: 261 µm Tests	P Value (one Tail)	Variance Variable 1	Variance Variable 2
2b (5.02% AL) - 4 (0% AL)	0.49	13.09	13.70
2b (5.02% AL) - 5 (10.04% AL)	0.06	13.09	0.87
4 (0% AL) - 5 (10.04% AL)	0.06	13.70	0.87

4.3.3 Burn Time

Table 20 shows results for motor burn time at each tested configuration for variations in ammonium perchlorate particle sizes and percentages of aluminum content. Calculation of burn duration was derived using the standard definition as defined in Figure 6 for each motor.

Table 20: Burn Time Performance for Variations in Ammonium Perchlorate Particle Size (Top) and Aluminum Content (Bottom)

Test	Average AP Particel Size (um)	Average Burn Time (s)	Average Burn Time (% Stdv)
1a	230	2.29	1.25%
1b	230	2.42	6.89%
2a	261	2.92	6.86%
2b	261	3.03	5.38%
3a	199	2.08	11.42%
3b	199	2.13	5.48%

Test	Total AP/AL Included (%)	Average Burn Time (s)	Average Burn Time (% Stdv)
4	80.82/0.00	2.71	11.60%
5	70.78/10.04	3.37	2.53%

A comparison of motor burn time against average ammonium perchlorate size appears to indicate that the two are directly proportional by what is observed in Figure 36. Higher average particle size resulted in longer burn times for both 3 grain and 2 grain motor configurations. A 78.78% direct correlation between burn time duration and ammonium perchlorate particle size was observed for 3 grain tests, while 2 grain tests produced an 86.48% linear correlation. This indicates a strong linear correlation between motor burn time and average ammonium perchlorate particle size.

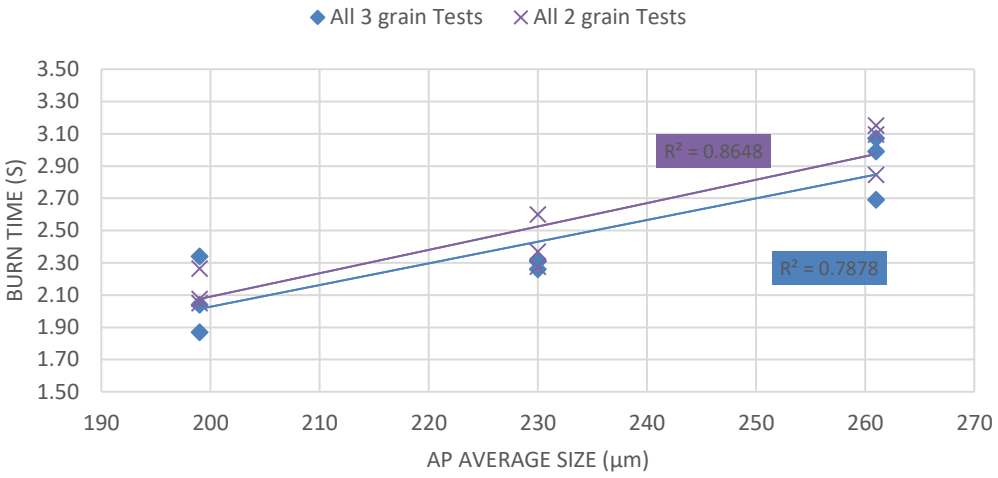

Figure 36: Burn Time vs. AP Average Size for All Tests

The second order polynomial curve fits in Figure 37 show averages of motor burn time against ammonium perchlorate particle size for 3 grain and 2 grain configurations that can be used in order to predict burn time duration.

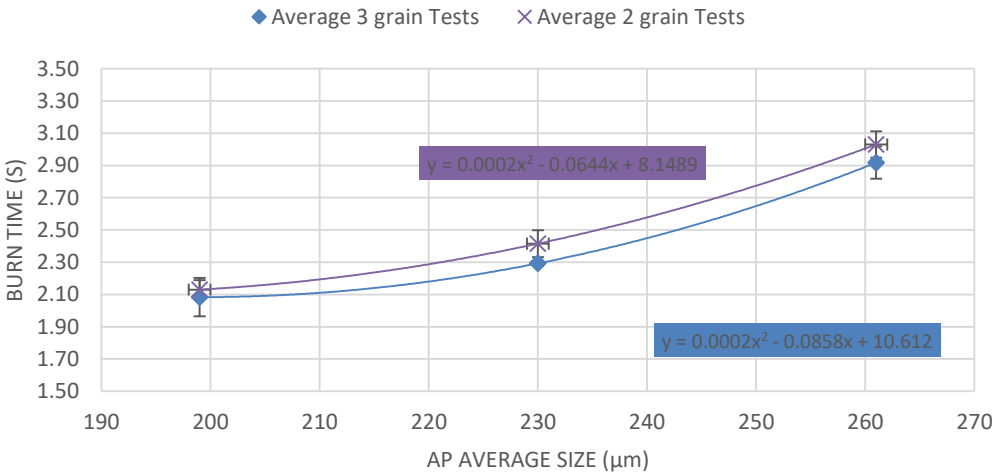

Figure 37: Average Burn Time vs. AP Average Size for All Tests

Figure 38 shows that a similar trend is observed for burn time duration as a function of ammonium perchlorate and aluminum content percentages. Motor burn time is observed to be inversely proportional to ammonium perchlorate content percentage and exhibited a 71.30% correlation for increasing ammonium perchlorate capturing a resulting decrease in burn time.

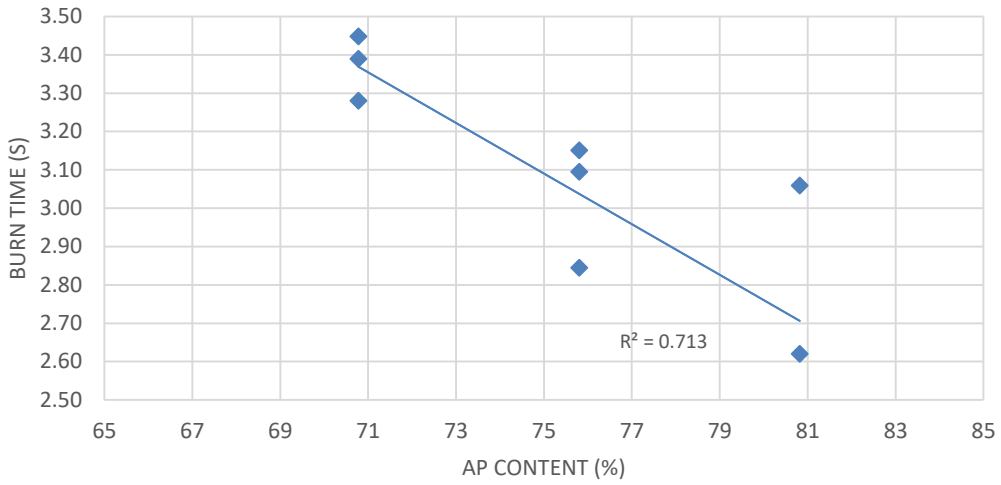

Figure 38: Burn Time vs. AP/AL Content Variation for All Tests

Figure 39 displays the second order polynomial curve fit for burn time duration against ammonium perchlorate content percentage that can be used in future modeling of burn time predictability.

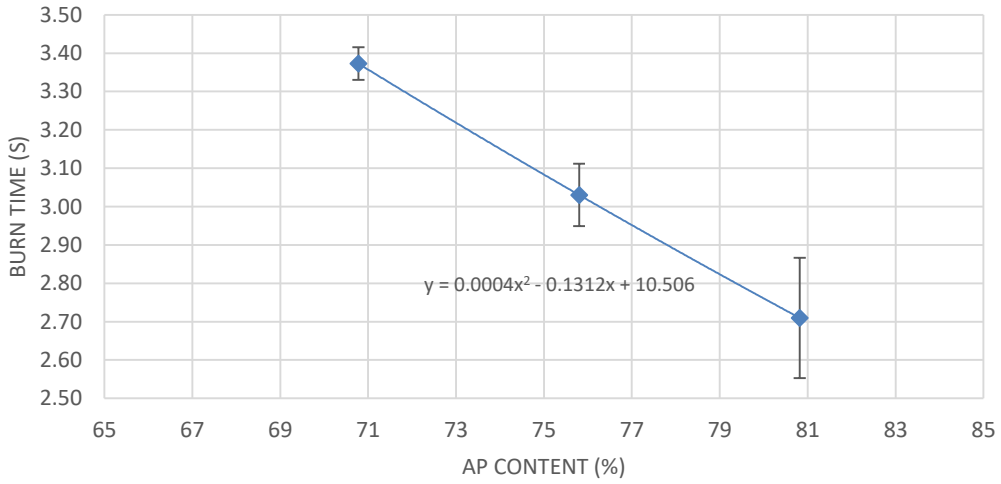

Figure 39: Average Burn Time vs. AP/AL Content Variation for All Tests

Hypothesis testing for burn time variance equality at each configured motor can be found in Table 21 through Table 24. When comparing 3 grain geometries at the varying average sizes of ammonium perchlorate particles, there were two significant differences in burn time variance. A

reduction in burn time variance was observed for 230 µm tests compared to those for 261 µm and 199 µm. No significant differences or evidence for significant differences in burn time variance was observed between 2 grain geometries at varying levels of average ammonium perchlorate particle size. In 3 versus 2 grain geometries a difference in burn time variance was detected for an ammonium perchlorate particle size of 230 µm, where a reduction in burn time variance is observed for 3 grain motors as compared to 2 grain motors. A potential variance reduction is noted at an ammonium perchlorate particle size of 199 µm, where 2 grain configurations were less variable than 3 grain. When aluminum and ammonium perchlorate content ratios were changed, variance testing showed a significant reduction in burn time variance at an aluminum weight fraction of 10.04% compared to an aluminum content formulation of 0%.

Table 21: Burn Time Equal Variance Results for 3 Grain Configured Motors at Equal AP Average Size

Comparison: 3 grain Geometries	P Value (one Tail)	Variance Variable 1	Variance Variable 2
1a (230 µm) - 2a (261 µm)	0.02	0.001	0.040
1a (230 µm) - 3a (199 µm)	0.01	0.001	0.057
2a (261 µm) - 3a (199 µm)	0.41	0.040	0.057

Table 22: Burn Time Equal Variance Results for 2 Grain Configured Motors at Equal AP Average Size

Comparison: 2 grain Geometries	P Value (one Tail)	Variance Variable 1	Variance Variable 2
1b (230 µm) - 2b (261 µm)	0.49	0.028	0.027
1b (230 µm) - 3b (199 µm)	0.33	0.028	0.014
2b (261 µm) - 3b (199 µm)	0.34	0.027	0.014

Table 23: Burn Time Equal Variance Results for 3 vs. 2 Grain Configured Motors at Equal AP Average Size

Comparison: 3 grain vs. 2 grain	P Value (one Tail)	Variance Variable 1	Variance Variable 2
1a (230 µm) - 1b (230 µm)	0.03	0.001	0.028
2a (261 µm) - 2b (261 µm)	0.40	0.040	0.027
3a (199 µm) - 3b (199 µm)	0.19	0.057	0.014

Table 24: Burn Time Equal Variance Results at a 261 µm AP Average Size for Varying AP/AL Content Ratios

Comparison: 261 µm Tests	P Value (one Tail)	Variance Variable 1	Variance Variable 2
2b (5.02% AL) - 4 (0% AL)	0.21	0.027	0.099
2b (5.02% AL) - 5 (10.04% AL)	0.22	0.027	0.007
4 (0% AL) - 5 (10.04% AL)	0.07	0.099	0.007

4.3.4 Total Impulse

Results for values of motor total impulse produced at each tested configuration for variations in average ammonium perchlorate particle size and percentages of aluminum content are shown in Table 25 below.

Table 25: Total Impulse Performance for Variations in Ammonium Perchlorate Particle Size (Top) and Aluminum Content (Bottom)

Test	Average AP Particel Size (um)	Total Impulse (lbf*s)	Total Impulse (% Stdv)
1a	230	199.18	8.32%
1b	230	206.91	6.65%
2a	261	211.40	9.80%
2b	261	208.84	2.38%
3a	199	199.27	5.12%
3b	199	194.99	1.81%

Test	Total AP/AL Included (%)	Total Impulse (lbf*s)	Total Impulse (% Stdv)
4	80.82/0.00	188.77	6.19%
5	70.78/10.04	193.52	2.08%

A comparison of motor total impulse against ammonium perchlorate size indicates a weak proportionality between the two, as observed in Figure 40. Higher average particle sizes gave slightly larger values of total impulse for both 3 grain and 2 grain motor configurations. A 11.55% direct correlation between total impulse magnitude and ammonium perchlorate particle size was observed for 3 grain tests, while 2 grain tests produced a 36.39% linear correlation.

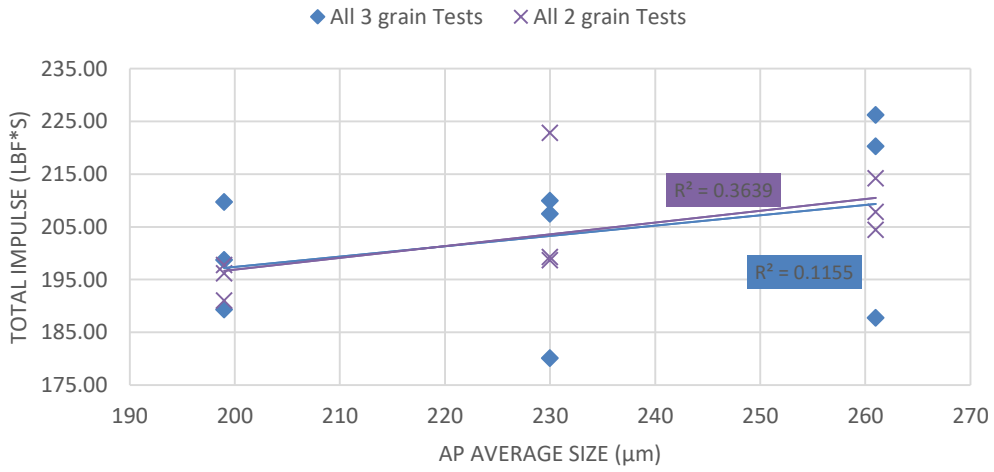

Figure 40: Total Impulse vs. AP Average Size for All Tests

However, this is not an unexpected result. If the overall content ratios of a propellant formulation remain the same, total impulse effectively becomes a measure of how much energy is packed within the motor itself. Thus, it should be more dependent on the mass capable of being within the geometry constraints of the motor casing, making total propellant mass of the motor a more suitable metric to observe trends related to total impulse. Upon observation of this, 73.98% of total impulse values were linearly correlated to propellant mass for 3 grain configurations, while 2 grain configurations produced a 62.10% correlation. This indicates the expected moderate-strong relationship between total impulse and motor propellant mass. Total impulse as a function of propellant mass can be observed in Figure 41 for all tests conducted at 75.80% and 5.02% concentrations of ammonium perchlorate and aluminum, respectively. It is important to note that one outlier for each 2 and 3 grain motor configuration was found and excluded from linear regression analysis results.

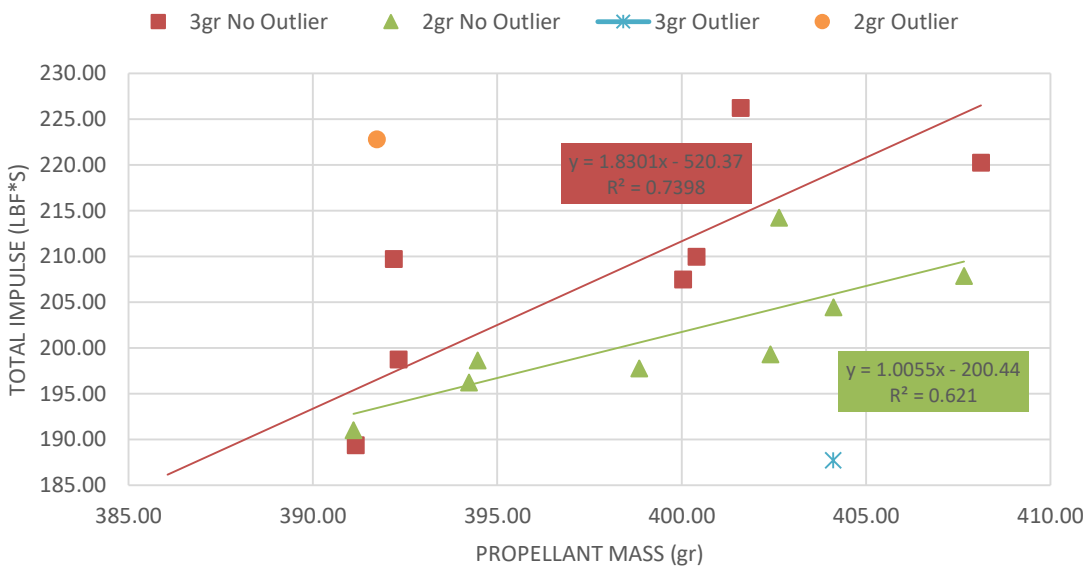

Figure 41: Total Impulse vs. Motor Propellant Mass for All Tests with 75.80% AP Content

Second order polynomial curve fits in Figure 42 show average motor total impulse against average ammonium perchlorate particle size for 3 grain and 2 grain configurations that can be used in order to predict magnitudes of total impulse in potential future studies.

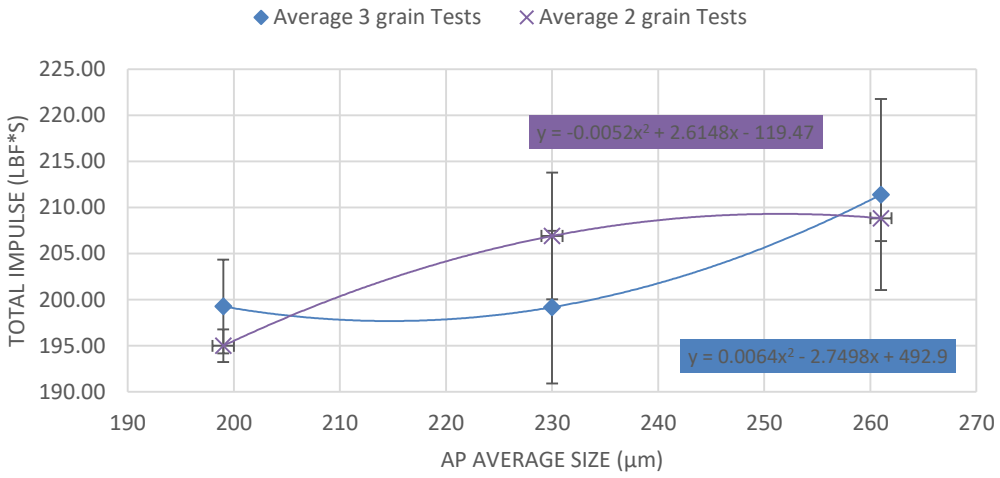

Figure 42: Average Total Impulse vs. AP Average Size for All Tests

The trend observed in Figure 43, showing total impulse as a function of ammonium perchlorate and aluminum content percentages, indicates that no linear trend exists between the two. Only a 3.34% correlation existed that supported a slight decrease in total impulse as ammonium perchlorate content increased. A comparison of total impulse against propellant mass at various ammonium perchlorate content percentages is not beneficial in this case as total formulation is not held constant, thus different values of total impulse are to be expected.

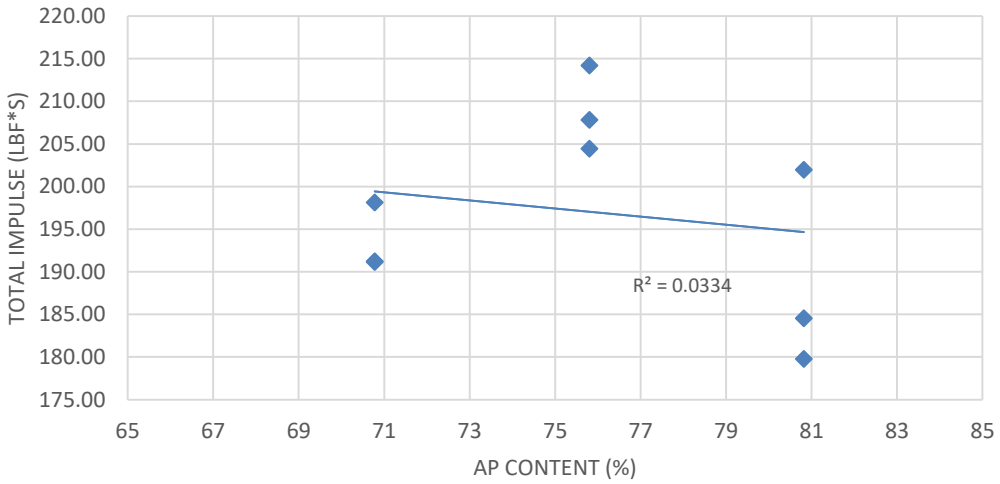

Figure 43: Total Impulse vs. AP/AL Content Variation for All Tests

Figure 44 displays the second order polynomial curve fit for total impulse against ammonium perchlorate content percentage that can be used in future modeling of total impulse predictability.

Total impulse maximized at an ammonium perchlorate content of 75.80%, and decreased both as ammonium perchlorate content was increased or decreased to 80.82% or 70.78%.

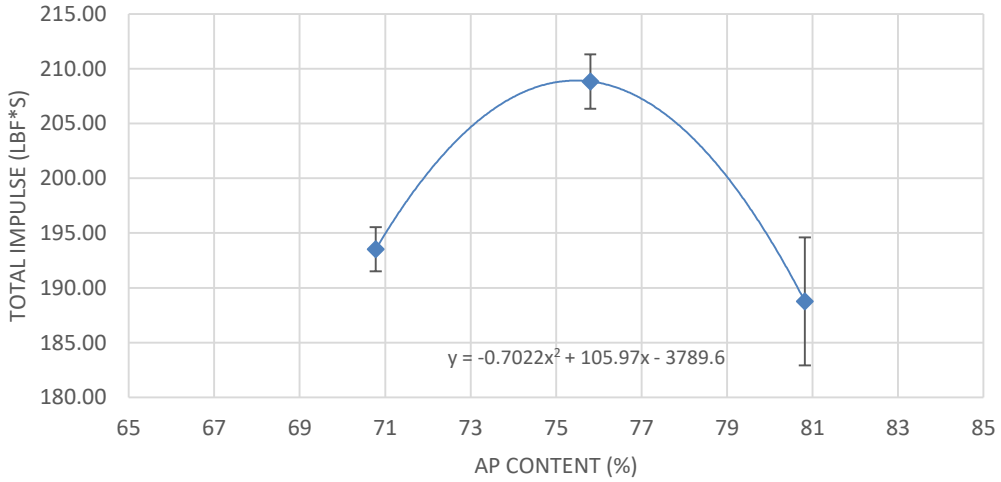

Figure 44: Average Total Impulse vs. AP/AL Content Variation for All Tests

Null-hypothesis testing procedures were applied to total impulse metrics in order to determine the presence of variance inequality as found in Table 26 through Table 29. When comparing 3 grain geometries at the varying sizes of ammonium perchlorate particles, there were no significant differences in total impulse variance. However, it should be noted that the potential for a decrease in total impulse variance could potentially exist for 199 µm sizes as compared to those of 261 µm. A significant difference is observed between a set of 2 grain geometries, where 199 µm tests varied less than 230 µm. Also, a near significant result was observed in the case of 261 µm sizes varying less than 230 µm. In 3 versus 2 grain geometries a difference in total impulse variance was detected for at an average ammonium perchlorate particle size of 261 µm, where a variance reduction is observed for 2 grain motors as compared to 3 grain motors. A potential variance reduction is noted at an average ammonium perchlorate particle size of 199 µm, where 2 grain configurations had less variable total impulse than 3 grain. A change in aluminum and ammonium perchlorate content ratios showed potential reductions in total impulse variance at an aluminum weight fraction of 10.04% compared to an aluminum content formulation of 0% and in an aluminum weight fraction of 5.02% compared to 0%.

Table 26: Total Impulse Equal Variance Results for 3 Grain Configured Motors at Equal AP Average Size

Comparison: 3 grain Geometries	P Value (one Tail)	Variance Variable 1	Variance Variable 2
1a (230 µm) - 2a (261 µm)	0.39	274.61	429.43
1a (230 µm) - 3a (199 µm)	0.27	274.61	103.94
2a (261 µm) - 3a (199 µm)	0.19	429.43	103.94

Table 27: Total Impulse Equal Variance Results for 2 Grain Configured Motors at Equal AP Average Size

Comparison: 2 grain Geometries	P Value (one Tail)	Variance Variable 1	Variance Variable 2
1b (230 µm) - 2b (261 µm)	0.12	189.28	24.61
1b (230 µm) - 3b (199 µm)	0.06	189.28	12.48
2b (261 µm) - 3b (199 µm)	0.34	24.61	12.48

Table 28: Total Impulse Equal Variance Results for 3 vs. 2 Grain Configured Motors at Equal AP Average Size

Comparison: 3 grain vs. 2 grain	P Value (one Tail)	Variance Variable 1	Variance Variable 2
1a (230 µm) - 1b (230 µm)	0.41	274.61	189.28
2a (261 µm) - 2b (261 µm)	0.05	429.43	24.61
3a (199 µm) - 3b (199 µm)	0.11	103.94	12.48

Table 29: Total Impulse Equal Variance Results at a 261 µm AP Average Size for Varying AP/AL Content Ratios

Comparison: 261 µm Tests	P Value (one Tail)	Variance Variable 1	Variance Variable 2
2b (5.02% AL) - 4 (0% AL)	0.15	24.61	136.40
2b (5.02% AL) - 5 (10.04% AL)	0.40	24.61	16.16
4 (0% AL) - 5 (10.04% AL)	0.11	136.40	16.16

4.3.5 Specific Impulse

Results for values of motor specific impulse produced at each tested configuration for variations in average ammonium perchlorate particle size and percentages of aluminum content are shown in Table 30 below.

Table 30: Specific Impulse Performance for Variations in Ammonium Perchlorate Particle Size (Top) and Aluminum Content (Bottom)

Test	Average AP Particel Size (um)	Specific Impulse (s)	Specific Impulse (% Stdv)
1a	230	228.24	6.34%
1b	230	237.01	7.70%
2a	261	237.01	9.87%
2b	261	234.02	2.73%
3a	199	230.63	4.99%
3b	199	224.06	0.99%

Test	Total AP/AL Included (%)	Specific Impulse (s)	Specific Impulse (% Stdv)
4	80.82/0.00	218.83	6.51%
5	70.78/10.04	215.51	1.80%

Motor specific impulse compared to average ammonium perchlorate sizes gives a very low direct proportionality similar to what was observed for total impulse, as shown in Figure 45. Higher particle sizes gave slightly larger values of specific impulse for both 3 grain and 2 grain motor configurations. A 3.21% direct correlation between total impulse magnitude and ammonium perchlorate particle size was observed for 3 grain tests, while 2 grain tests produced a 14.39% linear correlation. This weak correlation is expected as specific impulse is described as the total energy exerted per unit mass of the propellant formulation. Therefore, specific impulse is related to the propellant formulation itself.

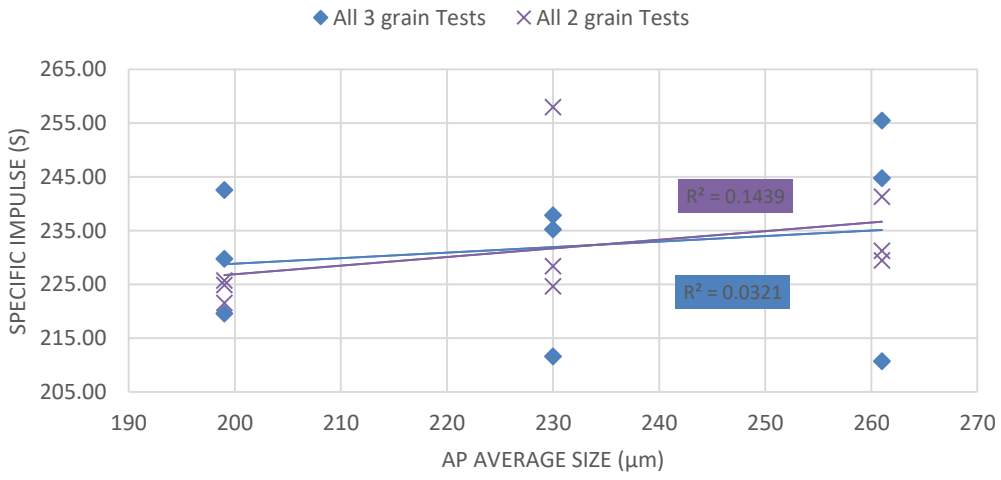

Figure 45: Specific Impulse vs. AP Average Size for All Tests

Figure 46 shows second order polynomial curve fits for average motor specific impulse against average ammonium perchlorate particle size for 3 grain and 2 grain configurations that can be used in order to predict magnitudes of specific impulse in potential future studies.

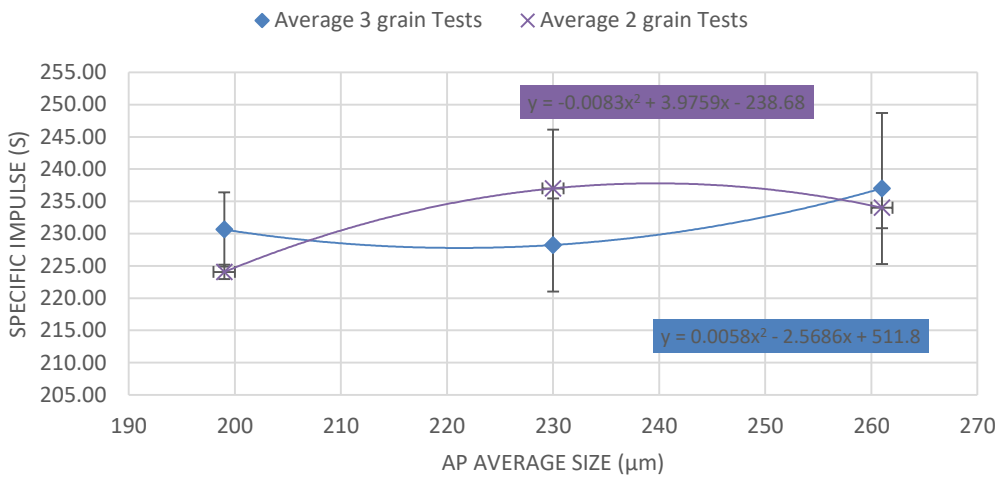

Figure 46: Average Specific Impulse vs. AP Average Size for All Tests

Observing Figure 47 gives no implications that a linear trend exists between specific impulse and ammonium perchlorate total content. Only a 1.5% correlation exists that supports a slight increase in specific impulse as ammonium perchlorate content is increased.

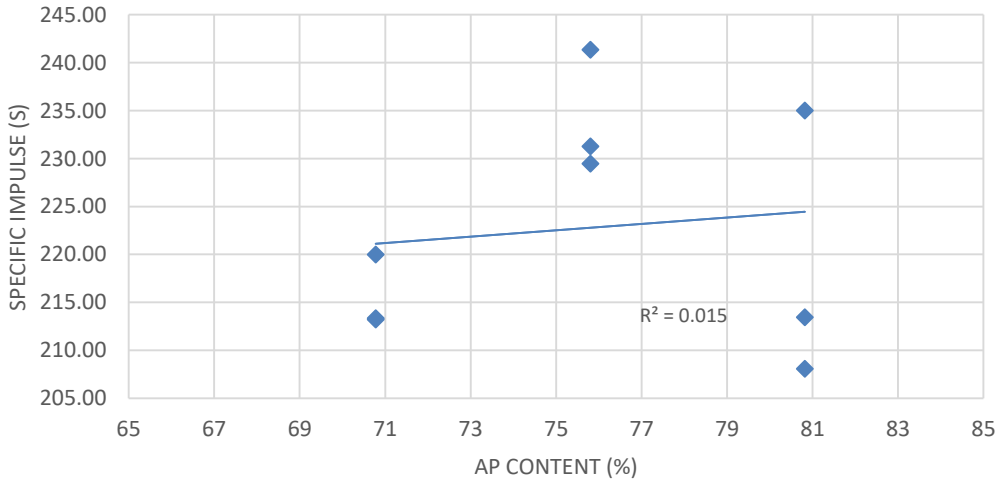

Figure 47: Specific Impulse vs. AP/AL Content Variation for All Tests

Figure 48 displays the second order polynomial curve fit for specific impulse against ammonium perchlorate content percentage that can be used in future modeling of total impulse predictability. Specific impulse trends followed those observed for total impulse when ammonium perchlorate content was varied as maximum average values were observed at 75.80%, with decreasing magnitudes appearing when content was increased or decreased to 80.82% and 70.78%.

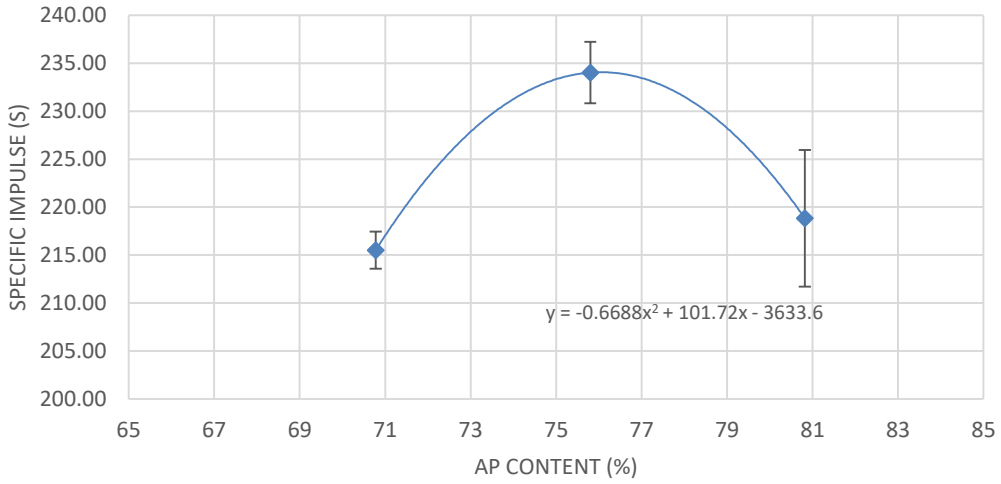

Figure 48: Specific Impulse vs. AP/AL Content Variation for All Tests

Hypothesis testing procedures were applied to values of specific impulse for each motor to perform the variance comparisons found in Table 31 through Table 34. When comparing 3 grain geometries at varying average sizes of ammonium perchlorate particles, there were no significant differences in specific impulse variance. A potential decrease in specific impulse variance could exist for 199 µm sizes as compared to those of 261 µm. All 2 grain geometries had either significant differences or the potential for a significant difference in specific impulse variance with varying ammonium perchlorate particle sizes. A significant reduction in variance was achieved in 199 µm tests when compared to those at 230 µm. Nearly significant differences were noted for a reduction in variance at 261 µm compared to 230 µm, as well as in the case for 199 µm compared to 261 µm. In 3 versus 2 grain geometries, a reduction in specific impulse variance was detected for at ammonium perchlorate particle sizes of 261 µm and 199 µm, where variance reductions are observed for 2 grain motors as compared to 3 grain motors. Changing

aluminum and ammonium perchlorate content ratios resulted in a reduction in specific impulse variance at an aluminum weight fraction of 10.04% compared to an aluminum content formulation of 0%. The potential for a variance reduction in an aluminum weight fraction of 5.02% compared to 0% is noted.

Table 31: Specific Impulse Equal Variance Results for 3 Grain Configured Motors at Equal AP Average Size

Comparison: 3 grain Geometries	P Value (one Tail)	Variance Variable 1	Variance Variable 2
1a (230 µm) - 2a (261 µm)	0.28	209.21	547.41
1a (230 µm) - 3a (199 µm)	0.39	209.21	132.59
2a (261 µm) - 3a (199 µm)	0.19	547.41	132.59

Table 32: Specific Impulse Equal Variance Results for 2 Grain Configured Motors at Equal AP Average Size

Comparison: 2 grain Geometries	P Value (one Tail)	Variance Variable 1	Variance Variable 2
1b (230 µm) - 2b (261 µm)	0.11	333.18	40.81
1b (230 µm) - 3b (199 µm)	0.01	333.18	4.97
2b (261 µm) - 3b (199 µm)	0.11	40.81	4.97

Table 33: Specific Impulse Equal Variance Results for 3 vs. 2 Grain Configured Motors at Equal AP Average Size

Comparison: 3 grain vs. 2 grain	P Value (one Tail)	Variance Variable 1	Variance Variable 2
1a (230 µm) - 1b (230 µm)	0.39	209.21	333.18
2a (261 µm) - 2b (261 µm)	0.07	547.41	40.81
3a (199 µm) - 3b (199 µm)	0.04	132.59	4.97

Table 34: Specific Impulse Equal Variance Results at a 261 µm AP Average Size for Varying AP/AL Content Ratios

Comparison: 261 µm Tests	P Value (one Tail)	Variance Variable 1	Variance Variable 2
2b (5.02% AL) - 4 (0% AL)	0.17	40.81	203.15
2b (5.02% AL) - 5 (10.04% AL)	0.27	40.81	14.98
4 (0% AL) - 5 (10.04% AL)	0.07	203.15	14.98

4.3.6 Ensemble Thrust Profile Analysis

In order to observe the consistency of thrust profiles achieved by each motor configuration, an ensemble average was taken for each motor at their differing average particle sizes, grain geometries, and ratios of ammonium perchlorate and aluminum content. Table 35 below displays average thrust profile percent deviations over the course of each motor's entire

burn. Additionally, a measure of how well each motor consistently met its ensemble average deviation is captured. This is done through taking the standard deviation of all the percent thrust deviations that occurred at each point represented in each ensemble thrust profile.

Table 35: Ensemble Thrust Profile Average Deviation and Deviation Consistency for Variations in Ammonium Perchlorate Particle Size (Top) and Aluminum Content (Bottom)

Test	Average AP Particel Size (um)	Ensemble Thrust Profile (Average % Stdv)	Deviation of Ensamble % Stdv (%)
1a	230	14.28%	11.16%
1b	230	19.85%	35.40%
2a	261	22.11%	21.82%
2b	261	9.73%	16.65%
3a	199	34.84%	38.68%
3b	199	21.32%	36.58%

Test	Total AP/AL Included (%)	Ensemble Thrust Profile (Average % Stdv)	Deviation of Ensamble % Stdv (%)
4	80.82/0.00	35.25%	32.32%
5	70.78/10.04	7.16%	14.55%

Form the table above, overall thrust profiles of 3 grain 230 µm motors deviated less than its 2 grain counter parts. In Figure 49 below, ensemble thrust profiles for 3 grain and 2 grain configured motors at a 230 µm ammonium perchlorate size can be viewed, with their error bars representing thrust standard deviation at each point throughout their burns. While average percent standard deviation for 3 and 2 grain configurations equal to 14.28% and 19.85%, respectively, the 3 grain motors also were able to maintain its 14.28% deviation value much more consistently than 2 grain motors. This is observed in that 3 grain percent standard deviation of the all the deviations making up the ensemble average sits at 11.16% while the 2 grain configurations come in at 35.40%. This trend appears to be consistent with Figure 49 as it is apparent that the amount of error around the 2 grain ensemble curve grows throughout the duration of its burn, while the 3 grain configuration remains fairly constant throughout.

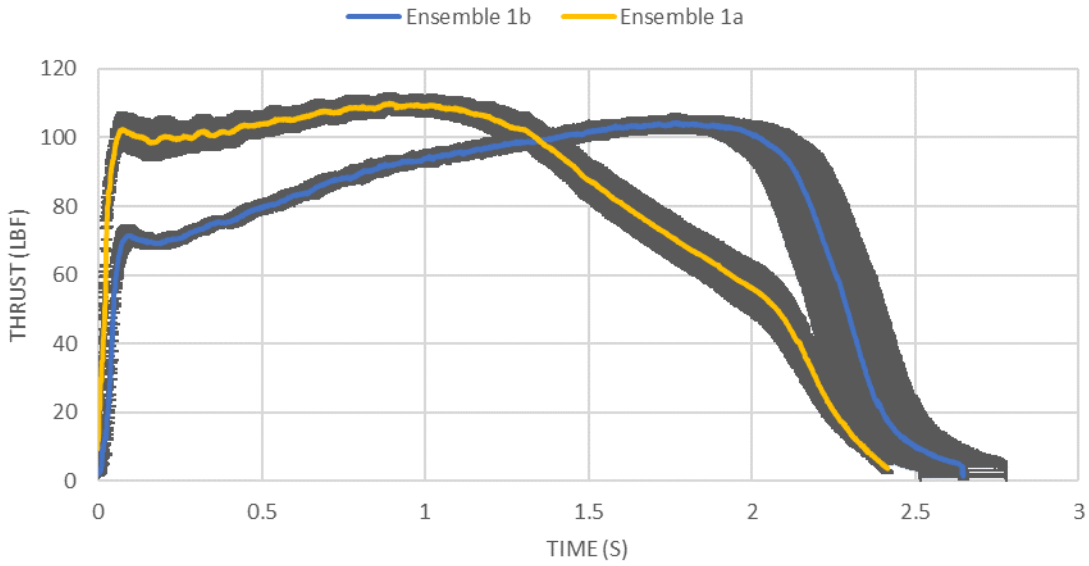

Figure 49: Ensemble Thrust Profiles for Motors at 230 µm AP Average Size for 2 Grain (1b) vs. 3 Grain (1a) Configurations

Figure 50 below displays ensemble thrust profiles for 3 grain and 2 grain configured motors at a 261 µm ammonium perchlorate size. Error bars representing thrust standard deviation at each point throughout their burns is displayed above and below each profile. Overall, average percent standard deviation and consistency of this deviation favored the 2 grain configuration more than the 3 grain configuration at an average ammonium perchlorate size of 261 µm. The 2 grain motors have an average thrust deviation equal to 9.73% while being able to maintain this average value within a standard deviation of 16.65%. Both of these values are improvements to the compared 3 grain 261 µm motors as they resulted in 22.11% and 21.82% values for average deviation and deviation consistency, respectively. Observation of these trends within Figure 50 is apparent in that the amount of error around the 2 grain ensemble cure is much smaller and less variable than in the 3 grain ensemble curve.

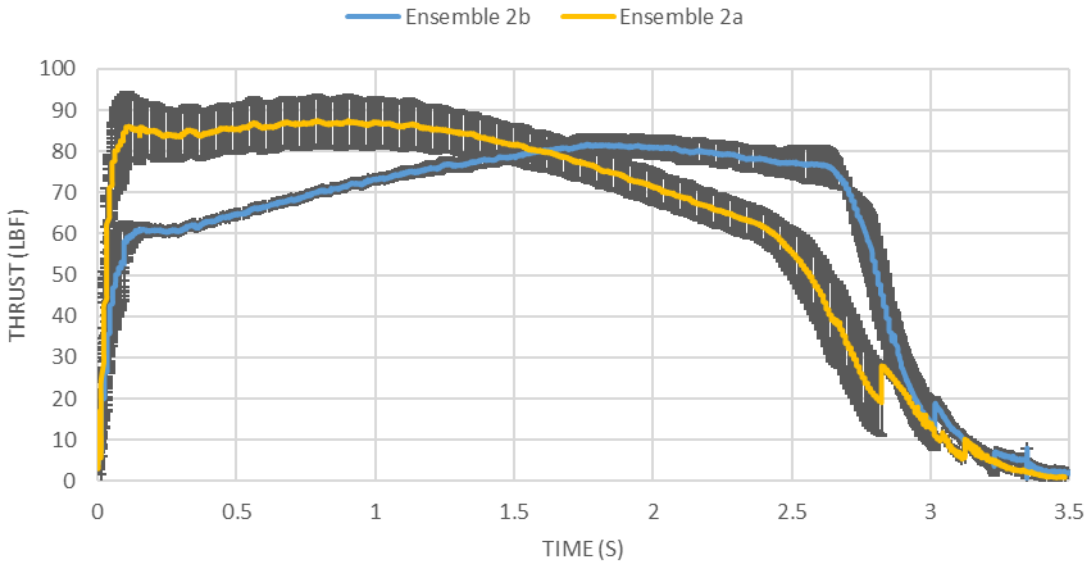

Figure 50: Ensemble Thrust Profiles for Motors at 261 µm AP Average Size for 2 Grain (2b) vs. 3 Grain (2a) Configurations

Ensemble thrust profiles for 3 grain and 2 grain configured motors at a 199 µm ammonium perchlorate average size are found in Figure 51, along with their error bars. Overall, average percent standard deviation and consistency of this deviation slightly favored the 2 grain configuration more than the 3 grain configuration at a 199 µm ammonium perchlorate average size. The 2 grain motors have an average thrust deviation equal to 21.32% while being able to maintain this average value within a standard deviation of 36.58%. Both of these values mentioned previously are better when compared to the 3 grain 199 µm motors as they resulted in 34.84% and 38.68% values of average deviation and deviation consistency, respectively. While 199 µm 2 grain and 3 grain motor ability to meet their average thrust deviation is very similar, 2 grain motors are able to exhibit this at a lower overall average percent thrust deviation. These trends are observed within Figure 51 through noting that error bars for the 199 µm 2 grain motors are smaller than that of 3 grain motor, but the error bars within each motor group vary similarly in relative magnitude to each other.

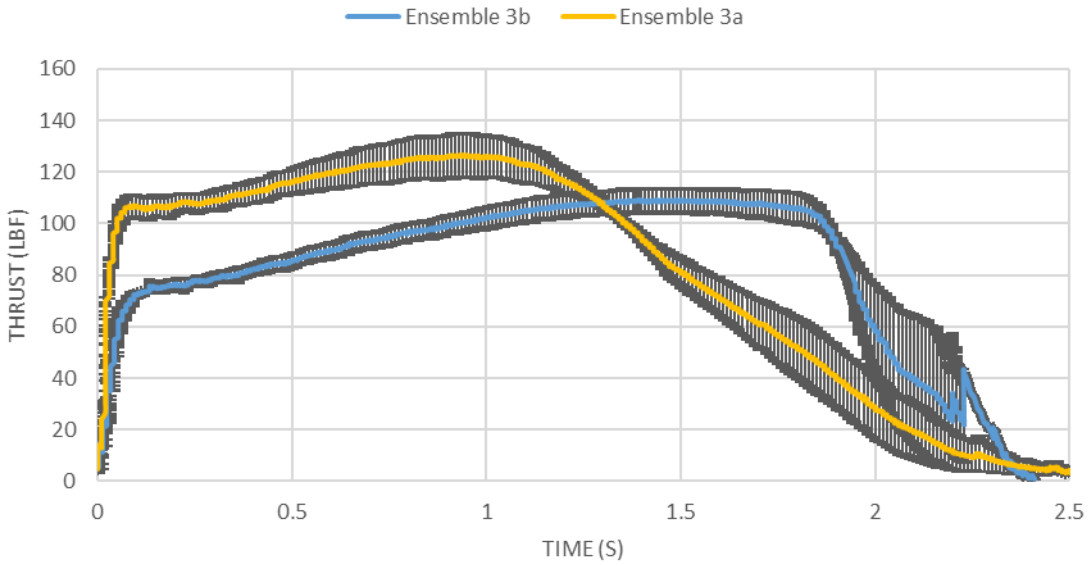

Figure 51: Ensemble Thrust Profiles for Motors at 199 µm AP Average Size for 2 Grain (3b) vs. 3 Grain (3a) Configurations

Ensemble thrust profiles for 2 grain configured motors at an ammonium perchlorate average size of 261 µm are found in Figure 52, where the total content ratio of ammonium perchlorate and aluminum was varied. Both percent average thrust profile deviation and the ability to consistently maintain this average deviation improved as total aluminum content decreased. When an aluminum content of 10.04% was tested, thrust profile average deviation and deviation consistency were at minimums, equaling 7.16% and 14.55% respectively. Conversely, both thrust profile average deviation and deviation consistency values were maximized when aluminum content was totally removed and reached values of 35.25%, and 32.32% respectively. Figure 52 shows this trend when it is observed that error bars grow both in magnitude and relative magnitude variance as total aluminum content is decreased.

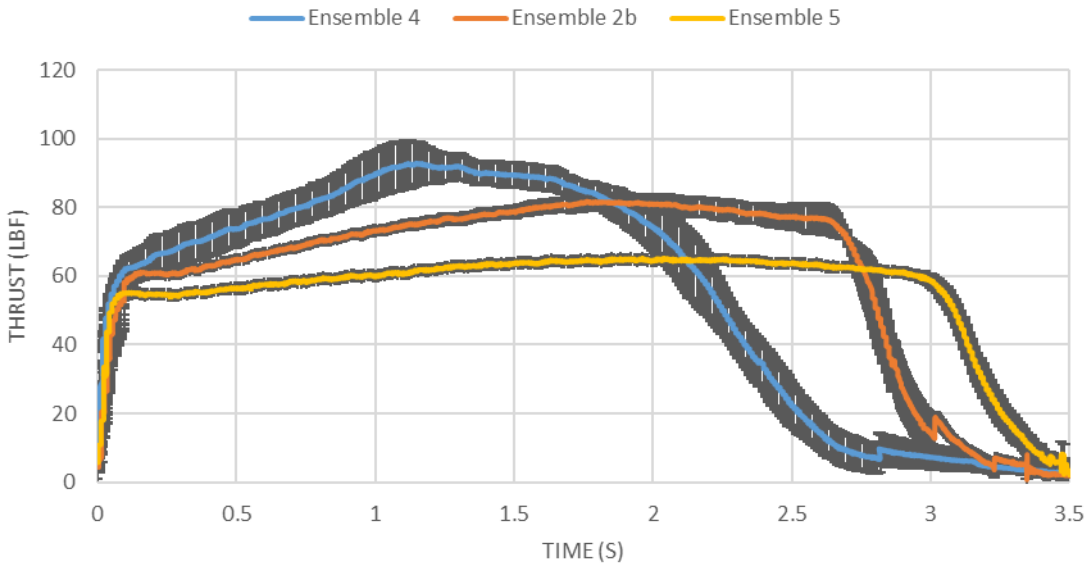

Figure 52: Ensemble Thrust Profiles for Motors at 261 µm AP Average Size with Varying AP/AL Content at 0% AL (4), 5.02% (2b), and 10.04% (5)

Figure 53 shows ensemble thrust profiles for 3 grain configured motors at differing ammonium perchlorate average sizes. Average thrust deviation and deviation consistency were most desirable at a 230 µm ammonium perchlorate size while maximum overall deviation and the least amount of consistency occurred at 199 µm tests.

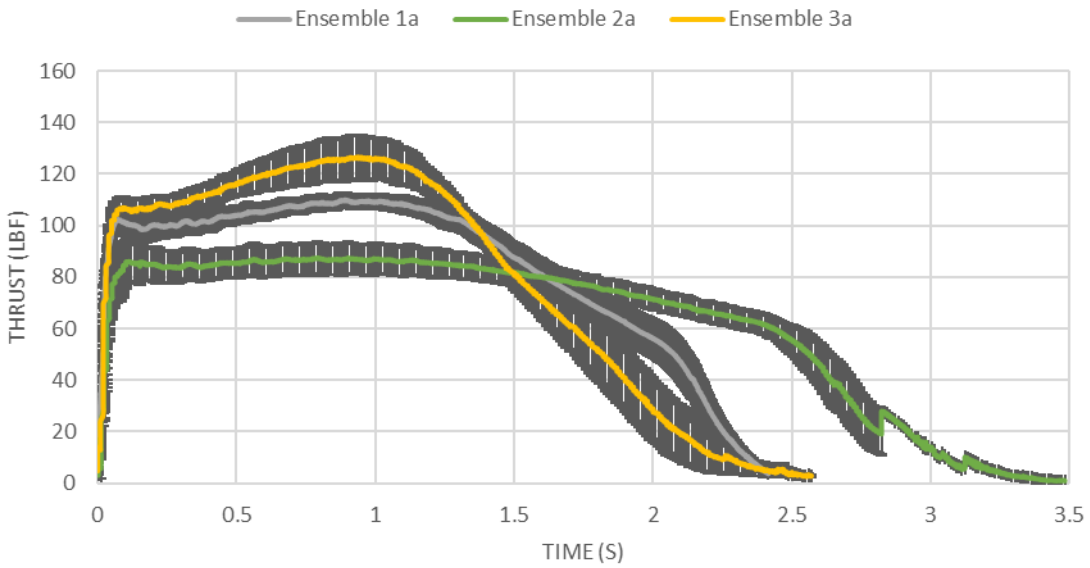

Figure 53: Ensemble Thrust Profiles for Motors in 3 Grain Configuration at Varying AP Particle Average Sizes of 230 µm (1a), 261 µm (2a), and 199 µm (3a)

Ensemble thrust profiles for 2 grain configured motors at differing ammonium perchlorate average sizes are shown in Figure 54. Average thrust deviation was minimized and deviation consistency was improved at a 261 µm ammonium perchlorate average size. Tests results for 2 grain varying ammonium perchlorate sizes equal to 199 µm and 230 µm exhibited very similar values of thrust deviations and consistency of that deviation. Both motors exhibit similar values with 230 µm tests having a slight advantage in both categories.

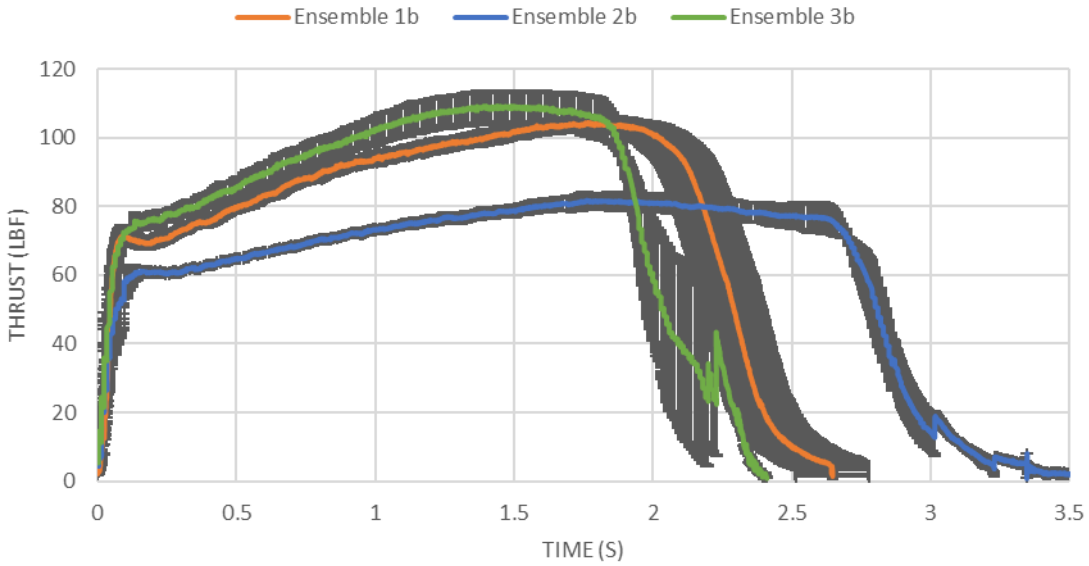

Figure 54: Ensemble Thrust Profiles for Motors in 2 Grain Configuration at Varying AP Particle Average Sizes of 230 µm (1b), 261 µm (2b), and 199 µm (3b)

CHAPTER V

CONCLUSIONS, OUTCOMES, AND RECCOMENDATIONS

5.1 General Performance Observations

As mentioned before, the primary goal of this study is to evaluate consistency of performance relative to changes in granular composition and propellant grain length, but several performance trends were also observed throughout this study. Both peak and average thrust exhibited a tendency to increase with a decrease in average ammonium perchlorate particle size, with the opposite being true for burn time. Both of these general trends correlate with the findings of other studies such as Thomas et. al., Rodić and Bajlovski, Park et al., and Babu et al. [32, 33, 11, 29]. All of these studies concluded an increase in burn rate with an increase in smaller ammonium perchlorate particle size concentration. Thus, when the ammonium perchlorate particle size is smaller, the propellant will tend to burn quicker due to the increased average particle surface area. This is easily observed through the use of Equations 6 & 7 showing an increase in burning surface area will result in an increased chamber pressure and therefore burn rate. Increased burn rate as a result of larger chamber pressures correlates to higher values of observed thrust that compensate for the reduced duration in burn time in order to maintain the same amount of total impulse that the propellant is capable of with the given amount of propellant mass in the motor. This can also be interpreted in the comparison of 3 grain verse 2 grain configured motors. Higher peak and average thrust values were continuously observed for 3 grain configurations, while longer burn times were concentrated to 2 grain configurations.

Increased burning surface areas are present in 3 grain motors as a larger grain count also results in two additional exposed surfaces on the ends of the extra grain. This increases total burning surface area which will again increase burn rate causing shortened burn times and increased thrust. Also, total and specific impulse remained nearly constant throughout all average ammonium perchlorate sizes which is expected. With no change in overall propellant ingredient percentages, the energy content relative to propellant mass should remain the same throughout.

An observed burn duration decrease with an ammonium perchlorate concentration increase is consistent with findings in Thomas et al. and Park et al. [32, 11]. A reduction in burn rate with decreased ammonium perchlorate concentration was observed as longer burn times were present when aluminum content was increased. This trend is less about burning surface area and more correlated to changes in chemical properties of the propellant that affect aspects such as density and characteristic velocity. This is indicated by total and specific impulse not remaining relatively constant across ammonium perchlorate total concentrations, meaning the energy available within the propellant is varying.

5.2 Research Objectives and General Outcomes

An analysis on solid rocket propellant performance consistency was performed. Several significant and potential significant differences have been attained between variances in average ammonium perchlorate particle size, ammonium perchlorate and aluminum content ratios, and propellant individual grain lengths. Key outcomes with respect to each core objective can be observed in sections 5.1.1 through 5.1.3 below.

5.2.1 Evaluation of AP Particle Size on Performance Consistency

Evaluation of ammonium perchlorate particle size impacts on performance consistency is captured through comparing performance results within classes of 3 grain and 2 grain motors. Beginning with motors in a 3 grain configuration, an average ammonium perchlorate particle size

of 230 µm was significantly less variable than 199 µm motors with respect to peak thrust, while also being less variable than both 199 µm and 261 µm motors for burn time. Motors with an ammonium perchlorate average particle size of 230 µm also were nearly significantly less variable than 261 µm motors in peak thrust. This trend changes slightly for parameters of total and specific impulse. While no significant differences were noted between average particle sizes, potential significance existed showing 199 µm motors varying less than 261 µm in both total and specific impulse. When ensemble profiles were observed, minimized deviation from ensemble thrust profile and highest consistency between each motor's thrust profile was achieved in 230 µm motors. The opposite of these trends is observed in 199 µm motors where maximum deviation and least amount of overall thrust profile consistency was observed.

Motors in a 2 grain configuration with varying ammonium perchlorate sizes showed distinct lower variations in average thrust values for 230 µm motors as compared to motors at 199 µm. Additionally, potentially significant reductions in variance is observed in 230 µm motors compared to 261 µm motors for both peak and average thrust. For total and specific impulse, significant reductions in performance variance is observed in 199 µm motors as compared to 230 µm motors. Potentially significant reductions are present in 261 µm configurations compared to its 230 µm counterparts for both specific and total impulse, while another potential variance reduction occurred between 199 µm and 261 µm motors for specific impulse where 199 µm varied less. Minimized ensemble deviation and best consistency of deviation was present in 261 µm motors, while 199 µm motors maximized average deviation and had the least amount of consistency with in the deviations that were present.

Small sample hypothesis testing and ensemble profile analysis shows a decrease in peak thrust, average thrust, and burn time variance at equal ratios of contributing ammonium perchlorate particle sizes. Conversely, consistency for specific and total impulse is increased when the concentration of small ammonium perchlorate particles is increased as shown through

hypothesis testing. Lastly, evidence suggests that all-around consistency can be balanced through an increase in larger ammonium perchlorate particle concentration. There are few instances where an increase in larger ammonium perchlorate particles are significantly more or less variable across all performance parameters. This apparent middle ground in performance consistency is supported with noting that minimized deviation and maximum consistency was present with an increase in larger particle size concentration within 2 grain motor ensemble profiles.

5.2.2 Evaluation of AP/AL Content on Performance Consistency

An evaluation on performance consistency relative to total amounts of ammonium perchlorate and aluminum content presented nearly significant unanimous observations in favor of motors with an increase in aluminum content. Motors where aluminum content percentages were maximized at 10.04% delivered significantly reduced variability in peak and average thrust when compared to 5.02% and 0% concentrations. A 10.04% aluminum concentration also resulted in potential reductions in variance when compared to 0% concentrations for metrics of burn time and total impulse. An additional significant reduction in specific impulse variance was observed for a 10.04% aluminum concentration compared to a 0% concentration. Potential reductions in 5.02% aluminum concentrations were noted for total and specific impulse as compared to a 0% aluminum concentration. These results coincide with decreased average ensemble deviations and best consistency within those deviations at the maximum aluminum concentration of 10.04%, while maximum average deviation and least amount of deviation consistency is present for 0% concentrations. Thus, hypothesis testing and ensemble analysis both support a reduction in performance variance with an increase in aluminum content.

5.2.3 Evaluation of Propellant Grain Length on Performance Consistency

Comparison of performance consistency between 2 grain and 3 grain configured motors at constant ammonium perchlorate particle sizes resulted in the majority of significant variation reductions being noted in 2 grain motors as compared to 3 grain. The only instance where 3 grain

variations were significantly or potentially significantly less than 2 grain motors was at a 230 μm ammonium perchlorate size where increased consistency was observed in motor burn time. A 261 μm average particle size resulted in significantly less variation with respect to metrics of total and specific impulse for 2 grain motors compared to 3 grain. Potentially significant variance reductions for 2 grain compared to 3 grain configurations at 261 μm were present for peak and average thrust. Motors at 199 μm average particle sizes varied significantly less for 2 grain motors compared to 3 grain for specific impulse. Also, 2 grain motors potentially could vary less at a 199 μm average particle size in metrics of burn time and total impulse. Another significant reduction in variance occurred in 230 μm motors where 2 grain motors were more consistent than 3 grain motors in average thrust produced. In analysis of ensemble thrust profiles, 261 μm and 199 μm motors had a reduction in average thrust deviation for 2 grain motors as compared to 3 grain. Also, 2 grain motors either had deviation consistency that was better than or equal to 3 grain motors within 261 μm and 199 μm configurations. The only example of decreased average ensemble profile deviation and improved deviation consistency for 3 grain motors as compared to 2 grain is present at an ammonium perchlorate average particle size equal to 230 μm. Thus, an increase in grain length generally will result in improved performance consistency.

5.3 Final Remarks and Recommendations

Evaluation of performance consistency relative to variations in granular size and grain length shows significant evidence towards a reduction in performance variation both as aluminum content and grain length is increased, i.e. as ammonium perchlorate content and total amount of propellant grains are decreased consistency is generally improved. Variation as a function of ammonium perchlorate particles shows that even contributions of particle sizes within a tri-modal composition gives a variability reduction in metrics of peak thrust, average thrust, and burn time. However, an increase in either larger or smaller particle concentration supports increased consistency with respect to total and specific impulse, with smaller average particle sized motors

having the least amount of variation for these two metrics. Tests for increased average particle size proved to be a slightly more all-around choice. This is shown in that reduced average particle size increased variability with respect to peak thrust, average thrust and burn time, while even contributions of ammonium perchlorate particles increased variability in total and specific impulse.

These trends in motor variance present the opportunity to assess a formulation's appropriateness to specific applications. It is apparent that if performance consistency alone is at the upmost importance, a decrease in number of grains with an increase in total aluminum content should be had to decrease the variability between motors. Increasing aluminum content will be the general choice for most applications both large and small scale where constraints related to burn duration, thrust, or total energy content are negotiable. When constraints related to burn time duration is required that would not allow for the longer burn times observed with a higher aluminum content, even ratios of ammonium perchlorate particle sizes would allow for less variability of motor burn time and thrust outputs. This would be especially desirable for RATO applications that are constrained to very short burn times and require higher ammonium perchlorate concentrations. Lastly, if the amount of total or specific impulse desired from the propellant formulation is constrained to a specified ammonium perchlorate and aluminum ratio, increase in small particle concentration will decrease the variability in total energy content within the motor. Total energy content consistency would be particularly desirable for larger scale applications when a particular destination or point is of interest, such as in intercontinental ballistic missiles.

This study has taken a rather broad approach to the issue of solid motor performance consistency. As a result, small sample sizes were used in order to integrate hypothesis testing that helped indicate significant variance reductions. A narrowed approach to the issue of motor variability would allow for increased testing to occur within selected configurations, thus

allowing for an increased level of confidence in results coming from equal variance comparisons. Also, the only data collection performed in this study were values of thrust produced against burn duration. Future studies should incorporate recording of chamber pressure to validate thrust profiles and analyze pressure variations that would have implications on solid rocket motor safety. Lastly, performance consistency has only been observed at a singular motor size diameter of 54 mm (2.13 in) with a 0.5 in tubular core at only three different ammonium perchlorate particle sizes. Studies at the standard neighboring motor sizes of 38 mm (1.50 in) and 76 mm (3.00 in) should be had in order to assess the applicability of these results to variable motor dimensions. Different core sizes and varying port geometries should be assessed on their affect towards performance consistency as well. Additionally, an increase in the diversity of the ammonium perchlorate particle sizes should be conducted to further observe the trends established within this study. On the subject of Oklahoma State University with regards to future advancements of their high powered rocketry program, this study allows for further solid rocket motor experimentation that can now expand to varying oxidizers, fuels, additives, and additive ratios to be further evaluated on performance and consistency.

REFERENCES

[1] Schabedoth, P. E. (2020). *Life cycle assessment of rocket launches and the effects of the propellant choice on their environmental performance* (thesis). Department of Energy and Process Engineering.

[2] Moody, K. J., Walsh, A. M., Ngo, A. D., Whyte, S., Stottlemyre, A., & Rouser, K. P. (2020). Development of sorbitol-based solid rocket motors for Propulsion Education. *AIAA Scitech 2020 Forum*. https://doi.org/10.2514/6.2020-0067

[3] Heister, S. D., Anderson, W. E., Pourpoint Thimotée, & Cassady, R. J. (2019). *Rocket Propulsion*. Cambridge University Press.

[4] Wikimedia Foundation. (2022, January 30). *Rocket engine nozzle*. Wikipedia. Retrieved April 4, 2022, from https://en.wikipedia.org/wiki/Rocket_engine_nozzle

[5] Mattingly, J. D., & Boyer, K. M. (2016). *Elements of propulsion: Gas turbines and rockets*. AIAA.

[6] STEINBERGER, R., & DRECHSEL, P. D. (1969). Manufacture of cast double-base propellant. *Advances in Chemistry*, 1–28. https://doi.org/10.1021/ba-1969-0088.ch001

[7] NASA. (n.d.). *Propellants*. NASA. Retrieved April 4, 2022, from https://history.nasa.gov/conghand/propelnt.htm

[8] Chaturvedi, S., & Dave, P. N. (2019). Solid propellants: AP/HTPB composite propellants. *Arabian Journal of Chemistry*, *12*(8), 2061–2068. https://doi.org/10.1016/j.arabjc.2014.12.033

[9] Lokiresearch.com. (n.d.). Retrieved April 4, 2022, from https://www.lokiresearch.com/default.aspx

[10] *Bureau of Alcohol, Tobacco, Firearms and Explosives*. Explosives Open Letters | Bureau of Alcohol, Tobacco, Firearms and Explosives. (2009, July 17). Retrieved April 4, 2022, from https://www.atf.gov/rules-and-regulations/explosives-open-letters

[11] Park, S., Choi, S., Kim, K., Kim, W., & Park, J. (2020). Effects of ammonium perchlorate particle size, ratio, and total contents on the properties of a composite solid propellant. *Propellants, Explosives, Pyrotechnics*, 45(9), 1376–1381. https://doi.org/10.1002/prep.202000055.

[12] Chaturvedi, S., & Dave, P. N. (2012). Cheminform abstract: Nano-metal oxide: Potential catalyst on thermal decomposition of ammonium perchlorate. *ChemInform*, *43*(21). https://doi.org/10.1002/chin.201221229

[13] Yang, V., Brill, T. B., & Ren, W.-Z. (2000). *Solid propellant chemistry, combustion, and Motor Interior Ballistics*. American Institute of Aeronautics and Astronautics.

[14] Boldyrev, V. V. (2006). Thermal decomposition of ammonium perchlorate. *Thermochimica Acta*, *443*(1), 1–36. https://doi.org/10.1016/j.tca.2005.11.038

[15] L. Bircomshaw, B. Newman, Thermal decomposition of ammonium perchlorate, Proc. Roy. Soc. A227 (1955) 228–237

[16] JACOBS, P. W., & RUSSELL-JONES, A. (1967). On the mechanism of the decomposition of ammonium perchlorate. *AIAA Journal*, *5*(4), 829–830. https://doi.org/10.2514/3.4085

[17] Pai Verneker, V. R., McCarty, M., & Maycock, J. N. (1971). Sublimation of ammonium perchlorate. *Thermochimica Acta*, *3*(1), 37–48. https://doi.org/10.1016/0040-6031(71)85055-4

[18] Meda, L., Marra, G., Galfetti, L., Severini, F., & De Luca, L. (2007). Nano-aluminum as energetic material for rocket propellants. *Materials Science and Engineering: C*, *27*(5-8), 1393–1396. https://doi.org/10.1016/j.msec.2006.09.030

[19] Galfetti, L., Luca, L. T., Severini, F., Meda, L., Marra, G., Marchetti, M., Regi, M., & Bellucci, S. (2006). Nanoparticles for solid rocket propulsion. *Journal of Physics: Condensed Matter*, *18*(33). https://doi.org/10.1088/0953-8984/18/33/s15

[20] Olivani, A., Galfetti, L., Severini, F., Colombo, G., Cozzi, F., Lesma, F., & Sgobba, M. (2002). Aluminum Particle Size Influence on Ignition and Combustion of AP/HTPB/Al Solid Rocket Propellants. Italy; Solid Propulsion Laboratory.

[21] Galfetti, L., DeLuca, L. T., Severini, F., Colombo, G., Meda, L., & Marra, G. (2007). Pre and post-burning analysis of nano-aluminized solid rocket propellants. *Aerospace Science and Technology*, *11*(1), 26–32. https://doi.org/10.1016/j.ast.2006.08.005

[22] Jain*, S. R. (2002). Solid Propellant Binders. *Journal of Scientific & Industrial Research*, *61*, 899–911.

[23] Sekkar, V., & Raunija, T. S. (2015). Hydroxyl-terminated polybutadiene-based polyurethane networks as solid propellant binder-state of the art. *Journal of Propulsion and Power*, *31*(1), 16–35. https://doi.org/10.2514/1.b35384

[24] Chaturvedi, S., & Dave, P. N. (2019). Solid propellants: AP/HTPB composite propellants. *Arabian Journal of Chemistry*, *12*(8), 2061–2068. https://doi.org/10.1016/j.arabjc.2014.12.033

[25] Pereira, C. A., Oliveira, F. G., & Villar, L. D. (2018). Association of Castor Oil and tepanol as a filler-binder bonding agent for solid rocket propellant. *2018 Joint Propulsion Conference*. https://doi.org/10.2514/6.2018-4576

[26] Dallas, J. A., Raval, S., Alvarez Gaitan, J. P., Saydam, S., & Dempster, A. G. (2020). The environmental impact of emissions from Space Launches: A comprehensive review. *Journal of Cleaner Production*, *255*, 120209. https://doi.org/10.1016/j.jclepro.2020.120209

[27] Naagar, M., & Chalia, S. (2017). Depletion of stratospheric ozone by chlorinated exhaust of ammonium perchlorate based composite solid propellant formulations: A review. *International Journal of Research in Advanced Engineering and Technology*, *3*(2), 01–05.

[28] Noaman, H., Ahmed, M., Abdalla, H., & Al-Sanabawy, M. (2013). Neutrality of taper-ended tubular grains. *International Conference on Aerospace Sciences and Aviation Technology*, *15*(AEROSPACE SCIENCES), 1–9. https://doi.org/10.21608/asat.2013.21877

[29] Suresh Babu, K. V., Kanaka Raju, P., Thomas, C. R., Syed Hamed, A., & Ninan, K. N. (2017). Studies on composite solid propellant with tri-modal ammonium perchlorate containing an ultrafine fraction. *Defence Technology*, *13*(4), 239–245. https://doi.org/10.1016/j.dt.2017.06.001

[30] Rocket Propulsion Elements – eighth edition G. P. Sutton and O. Biblarz John Wiley and Sons, the atrium, Southern Gate, Chichester, West Sussex, PO19 8SQ, UK, 2010. 768PP. illustrated. £90. ISBN 978-0-470-08024-5. (2011). *The Aeronautical Journal*, *115*(1163), 65. https://doi.org/10.1017/s0001924000005418

[31] Park, S., Won, J., Park, J., Park, E., & Choi, S. (2018). Solid propellants for propulsion system including a yellow iron oxide. *Journal of the Korean Society of Propulsion Engineers*, *22*(3), 65–71. https://doi.org/10.6108/kspe.2018.22.3.065

[32] Thomas, J. C., Morrow, G. R., Dillier, C. A., & Petersen, E. L. (2020). Comprehensive study of ammonium perchlorate particle size/concentration effects on propellant combustion. *Journal of Propulsion and Power*, *36*(1), 95–100. https://doi.org/10.2514/1.b37485

[33] Rodic, V., & Bajlovaski, M. (2006). Influence of Trimodal Fraction Mixture of Ammonium-Perchlorate on Characteristics of Composite Rocket Propellants. *Scientific-Technical Review*, *1*(2).

[34] Utley, L. (2020). *Coolant Passage Segmentation Influence On Regenerative-Cooling Effectiveness For Small Spacecraft Thrusters* (thesis).

[35] Utley, L., Foster, G., and Rouser, K., "Design and Evaluation of a Portable, Flexible-Use Rocket Thrust Stand," , 2017. Unpublished Manuscript.

[36] *Load button with Threaded/tapped holes - FUTEK*. futek. (n.d.). Retrieved April 5, 2022,

from https://media.futek.com/content/futek/files/pdf/productdrawings/llb400.pdf

[37] *High Power Rocket Safety Code effective August 2012*. National Association of Rocketry. (n.d.). Retrieved April 5, 2022, from https://www.nar.org/safety-information/high-power-rocket-safety-code/

APPENDICES

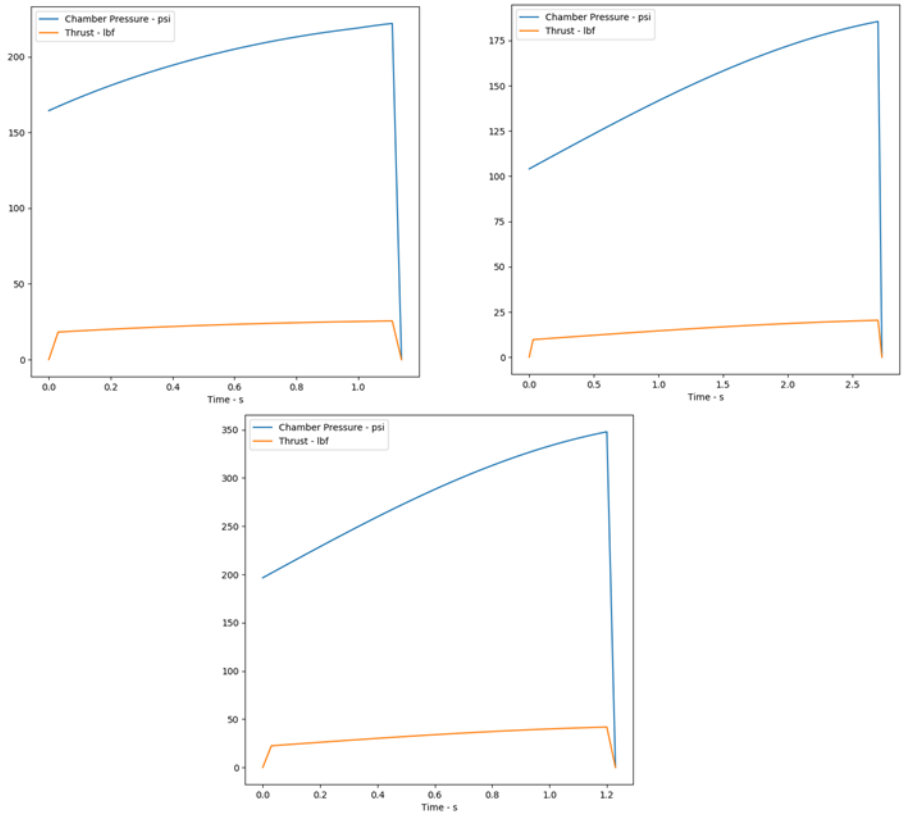

A.1: 38mm Simulations for KNSB (Left), APCP Cherry Limeade (Right) & APCP Blue Thunder (Bottom)

	Composition Variable	Test #	AP % 90	AP % 200	AP % 400	AP % Tot	AL % Tot	Total Grain #	L per Grain (in)	Prop Total L (in)
	AP Equal	1.1a	25.27	25.27	25.27	75.80	5	3	2.225	6.675
		1.2a	25.27	25.27	25.27	75.80	5	3	2.225	6.675
		1.3a	25.27	25.27	25.27	75.80	5	3	2.225	6.675
		1.4b	25.27	25.27	25.27	75.80	5	2	3.3375	6.675
		1.5b	25.27	25.27	25.27	75.80	5	2	3.3375	6.675
Config. 1 Total:	6	1.6b	25.27	25.27	25.27	75.80	5	2	3.3375	6.675
	AP90 - 10%	2.1a	15.27	25.27	35.27	75.80	5	3	2.225	6.675
		2.2a	15.27	25.27	35.27	75.80	5	3	2.225	6.675
		2.3a	15.27	25.27	35.27	75.80	5	3	2.225	6.675
		2.4b	15.27	25.27	35.27	75.80	5	2	3.3375	6.675
		2.5b	15.27	25.27	35.27	75.80	5	2	3.3375	6.675
Config. 2 Total:	6	2.6b	15.27	25.27	35.27	75.80	5	2	3.3375	6.675
	AP90 + 10%	3.1a	35.27	25.27	15.27	75.80	5	3	2.225	6.675
		3.2a	35.27	25.27	15.27	75.80	5	3	2.225	6.675
		3.3a	35.27	25.27	15.27	75.80	5	3	2.225	6.675
		3.4b	35.27	25.27	15.27	75.80	5	2	3.3375	6.675
		3.5b	35.27	25.27	15.27	75.80	5	2	3.3375	6.675
Config. 3 Total:	6	3.6b	35.27	25.27	15.27	75.80	5	2	3.3375	6.675
	PICK ONE FROM ABOVE									
	Composition Variable	Test #	AP % 90	AP % 200	AP % 400	AP % Tot	AL % Tot	Total Grain #	L per Grain (in)	Prop Total L (in)
	AL - 5%	4.1	TBD	TBD	TBD	80.82	0	TBD	TBD	6.675
		4.2	TBD	TBD	TBD	80.82	0	TBD	TBD	6.675
Config. 4 Total:	3	4.3	TBD	TBD	TBD	80.82	0	TBD	TBD	6.675
	AL + 5.0%	5.1	TBD	TBD	TBD	70.78	10	TBD	TBD	6.675
		5.2	TBD	TBD	TBD	70.78	10	TBD	TBD	6.675
Config. 5 Total:	3	5.3	TBD	TBD	TBD	70.78	10	TBD	TBD	6.675
Grand Total:	24									

A.2: Preliminary Motor Matrix

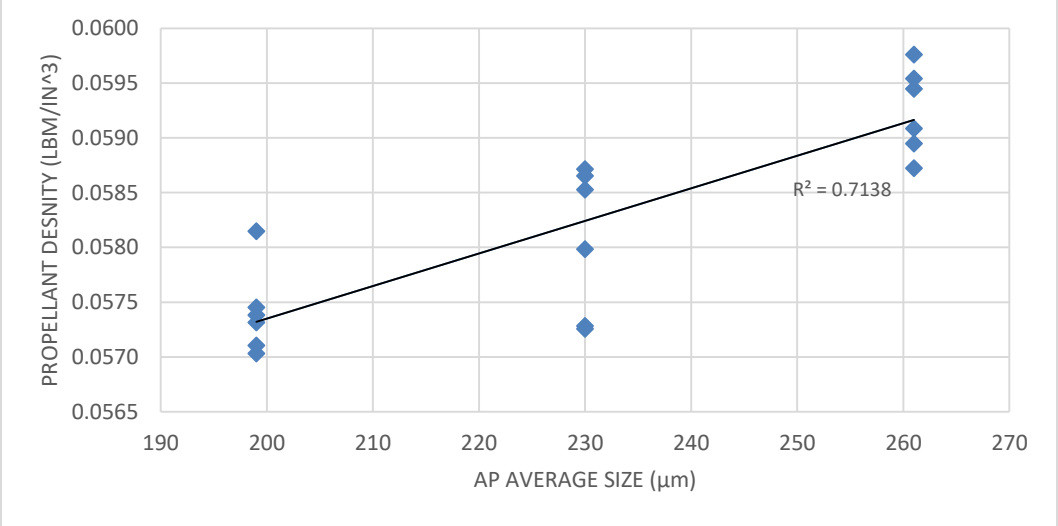

A.3: Propellant Density vs. AP Particle Average Size with Linear Trend Line

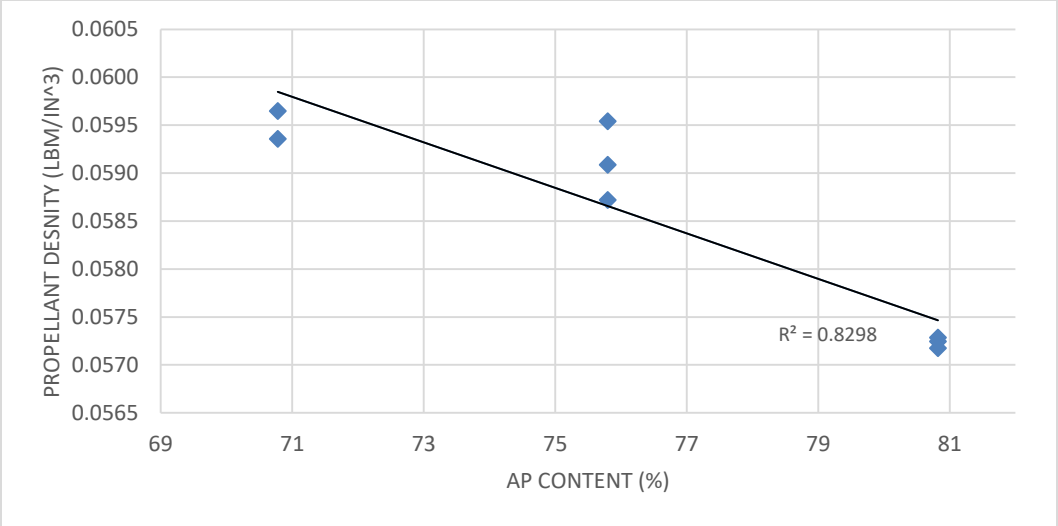

A.4: Propellant Density vs. AP/AL Total Content with Linear Trend Line

VITA

Daniel Velasco

Candidate for the Degree of

Master of Science

Thesis: EVALUATION OF GRANULAR DISTRIBUTION AND PROPELLANT GRAIN LENGTH ON TRI-MODAL AMMONIUM PERCHLORATE SOLID ROCKET MOTORS

Major Field: Mechanical and Aerospace Engineering

Biographical:

Education:

Completed the requirements for the Master of Science in Mechanical and Aerospace Engineering at Oklahoma State University, Stillwater, Oklahoma in May, 2022.

Completed the requirements for the Bachelor of Science in Mechanical and Aerospace Engineering at Oklahoma State University, Stillwater, Oklahoma in May, 2020.

Experience:

Graduate Research Assistant – Oklahoma State University, Stillwater, OK
Graduate Teaching Assistant – Oklahoma State University, Stillwater, OK

Professional Memberships:

Tau Beta Pi – Oklahoma State University, Stillwater, OK